



NAVAL POSTGRADUATE SCHOOL

MONTEREY, CALIFORNIA

THESIS

**A NOVEL PHOTOVOLTAIC POWER CONVERTER
FOR MILITARY AND SPACE APPLICATIONS**

by

Randyll R. M. Fernandez, Jr.

September 2005

Thesis Advisor:
Second Reader:

Sherif Michael
Robert Ashton

Approved for public release; distribution is unlimited

THIS PAGE INTENTIONALLY LEFT BLANK

REPORT DOCUMENTATION PAGE			<i>Form Approved OMB No. 0704-0188</i>
Public reporting burden for this collection of information is estimated to average 1 hour per response, including the time for reviewing instruction, searching existing data sources, gathering and maintaining the data needed, and completing and reviewing the collection of information. Send comments regarding this burden estimate or any other aspect of this collection of information, including suggestions for reducing this burden, to Washington headquarters Services, Directorate for Information Operations and Reports, 1215 Jefferson Davis Highway, Suite 1204, Arlington, VA 22202-4302, and to the Office of Management and Budget, Paperwork Reduction Project (0704-0188) Washington DC 20503.			
1. AGENCY USE ONLY (Leave blank)	2. REPORT DATE September 2005	3. REPORT TYPE AND DATES COVERED Master's Thesis	
4. TITLE AND SUBTITLE: A Novel Photovoltaic Power Converter For Military and Space Applications			5. FUNDING NUMBERS
6. AUTHOR(S) Fernandez, Randyll R.M. Jr.			
7. PERFORMING ORGANIZATION NAME(S) AND ADDRESS(ES) Naval Postgraduate School Monterey, CA 93943-5000			8. PERFORMING ORGANIZATION REPORT NUMBER
9. SPONSORING /MONITORING AGENCY NAME(S) AND ADDRESS(ES) N/A			10. SPONSORING/MONITORING AGENCY REPORT NUMBER
11. SUPPLEMENTARY NOTES: The views expressed in this thesis are those of the author and do not reflect the official policy or position of the Department of Defense or the U.S. Government.			
12a. DISTRIBUTION / AVAILABILITY STATEMENT Approved for public release; distribution is unlimited.			12b. DISTRIBUTION CODE
13. ABSTRACT (maximum 200 words) The purpose of this thesis is to consider PhotoVoltaic Power Converter (PVPC) technology, developed by Aтира Technologies®, and its prospects for military and space applications. This research will validate the hypothesis that PVPC technology enables a solar power system to produce usable power during low- and no-light conditions which standard solar power systems fail to provide. Solar cell panels are exposed to sunlight at different angles and with variable intensity, therefore the resulting output power varies depending on the illumination angle as well as the light intensity of each panel. Aтира Technologies® devised a novel buck-boost converter that is specifically designed to track the maximum power point of each solar panel. This would provide a significant increase in the overall available power by utilizing a switching topology in a subdued lighting condition. Although a small amount of power is generated, given enough time, a battery will reach its full charge, compared to no additional charging if the battery is using a panel without the circuit. In addition, this research will also show the vital sustaining information to substantiate PVPC's claim of usefulness and effectiveness to allow for longer time on station both in the field and in space so it can extend its missions.			
14. SUBJECT TERMS: Solar cells, photovoltaic power converter, I-V curve, NPSAT1, back-up power			15. NUMBER OF PAGES 97
			16. PRICE CODE
17. SECURITY CLASSIFICATION OF REPORT Unclassified	18. SECURITY CLASSIFICATION OF THIS PAGE Unclassified	19. SECURITY CLASSIFICATION OF ABSTRACT Unclassified	20. LIMITATION OF ABSTRACT UL

NSN 7540-01-280-5500

Standard Form 298 (Rev. 2-89)
Prescribed by ANSI Std. Z39-18

THIS PAGE INTENTIONALLY LEFT BLANK

Approved for public release; distribution is unlimited

**A NOVEL PHOTOVOLTAIC POWER CONVERTER FOR MILITARY AND
SPACE APPLICATIONS**

Randyll R M. Fernandez, Jr.
Lieutenant, United States Navy
B.S., Batangas State University, Philippines, 1989

Submitted in partial fulfillment of the
requirements for the degree of

MASTER OF SCIENCE IN ELECTRICAL ENGINEERING

from the

**NAVAL POSTGRADUATE SCHOOL
September 2005**

Author: Randyll R.M. Fernandez, Jr.

Approved by: Sherif Michael
Thesis Advisor

Robert W. Ashton
Second Reader

Jeffrey B. Knorr
Chairman, Department of Electrical and Computer Engineering

THIS PAGE INTENTIONALLY LEFT BLANK

ABSTRACT

The purpose of this thesis is to consider PhotoVoltaic Power Converter (PVPC) technology, developed by Atira Technologies®, and its prospects for military and space applications. This research will validate the hypothesis that PVPC technology enables a solar power system to produce usable power during low- and no-light conditions which standard solar power systems fail to provide. Solar cell panels are exposed to sunlight at different angles and with variable intensity, therefore the resulting output power varies depending on the illumination angle as well as the light intensity of each panel. Atira Technologies® devised a novel buck-boost converter that is specifically designed to track the maximum power point of each solar panel. This would provide a significant increase in the overall available power by utilizing a switching topology in a subdued lighting condition. Although a small amount of power is generated, given enough time, a battery will reach its full charge, compared to no additional charging if the battery is using a panel without the circuit. In addition, this research will also show the vital sustaining information to substantiate PVPC's claim of usefulness and effectiveness to allow for longer time on station both in the field and in space so it can extend its missions.

THIS PAGE INTENTIONALLY LEFT BLANK

TABLE OF CONTENTS

I.	INTRODUCTION.....	1
	A. BACKGROUND	1
	B. RESEARCH OBJECTIVES.....	1
	C. RESEARCH QUESTIONS.....	1
	1. Primary Research Question.....	1
	2. Secondary Research Questions.....	2
	D. SCOPE AND ORGANIZATION	2
	E. METHODOLOGY	2
	F. EXPECTED BENEFITS.....	2
II.	BASIC FUNDAMENTAL OF PHOTOVOLTAIC.....	3
	A. SOLAR CONSTANT, IRRADIANCE, AND AIR MASS NUMBER.....	3
	B. SOLAR CELLS.....	5
	1. Light Absorption and Material Selection	5
	2. Generation of Current.....	7
	3. Solar Cells Characterization.....	7
	4. Factors Affecting the Solar Cell Output	11
	5. Multi-Junction Solar Cells	13
	C. TERRESTRIAL AND SPACE SOLAR CELLS	14
III.	BASIC PRINCIPLE OF POWER CONVERTERS.....	17
	A. DC-DC CONVERTER BASICS.....	18
	1. Buck Converter/Step-Down Converter.....	18
	a. <i>Transition Between Continuous and Discontinuous.....</i>	<i>20</i>
	b. <i>Voltage Ratio of Buck Converter (Discontinuous Mode).....</i>	<i>20</i>
	2. Boost Converter Step-Up Converter	22
	3. Buck-Boost Converter	24
	B. CONVERTER COMPARISON	25
	C. OTHER CONVERTERS	25
	1. Cuk Converter.....	25
	2. Isolated DC-DC Converters.....	27
	3. Flyback Converter	27
	4. Forward Converter.....	28
IV.	DATA ANALYSIS.....	31
	A. INTRODUCTION.....	31
	B. TEST ANALYSIS	31
	1. Uni-Solar LM-3 Test.....	32
	2. LM-3 Test with Programmable Fixed Load.....	36
	C. SUMMARY OF THE TESTS.....	38
V.	MILITARY APPLICATIONS	39
	A. INTRODUCTION.....	39

B.	SOLDIER POWER REQUIREMENT	39
a.	<i>Typical Equipment</i>	44
b.	<i>Equipment That Uses the BA-5590 or Equivalent</i>	44
c.	<i>Battery Chargers</i>	47
C.	PERPETUAL AIRPLANE	49
1.	Limitations	49
2.	Improvements	50
D.	UNMANNED AERIAL VEHICLES (UAV)	51
E.	OTHER USES	53
F.	SUMMARY	54
VI.	SPACE APPLICATIONS	55
A.	INTRODUCTION	55
B.	SPACECRAFT ARCHITECTURE	55
C.	ON BOARD SUBSYSTEMS	56
1.	Command and Data Handler (C&DH) Subsystem	57
2.	Electrical Power Subsystem	57
3.	Attitude Control Subsystem	58
4.	Radio Frequency Subsystem	58
D.	PAYLOAD/MISSION EXPERIMENTS	58
1.	CERTO and Langmuir Probes	58
2.	Configurable Fault-Tolerant Processor (CFTP)	59
3.	Visible Wavelength Imager (VISIM)	59
4.	Solar-Cell Measurement System (SMS)	59
E.	POWER SOURCES	60
1.	Lithium-Ion Batteries	60
2.	Improved Triple Junction Solar Cells	61
F.	AS A RESERVE BACKUP POWER	65
G.	CONVERTER DESIGN	68
H.	SUMMARY	70
VII.	CONCLUSION	71
A.	INTRODUCTION	71
B.	CONCLUSIONS	71
1.	Primary Research Question:	71
2.	Secondary Research Questions:	71
C.	RECOMMENDATIONS	72
1.	Recommendations for Future Research	72
	LIST OF REFERENCES	73
	INITIAL DISTRIBUTION LIST	77

LIST OF FIGURES

Figure 1.	Illustration of the air mass number, path lengths, and zenith angles [From Ref 4].	5
Figure 2.	Output current-voltage relationship for a $p-n$ junction when dark and illuminated [After Ref 5].	9
Figure 3.	A sample $I-V$ curve for a solar cell with properties marked. In this example, the curve is for a triple-junction solar cell [After Ref 23].	9
Figure 4.	Circuit symbol for the solar cell. Note the current direction [From Ref 10].	11
Figure 5.	The effect of temperature on the solar cell's output. Increasing temperature will decrease the open-circuit voltage, while slightly raising the short circuit current [From Ref 11].	12
Figure 6.	Typical $I-V$ curves for the various single-junction cell technologies [From Ref 11].	13
Figure 7.	Simplified cross-sectional view of Improved Triple Junction Solar Cell Layers [From Ref 27].	14
Figure 8.	A Photovoltaic solar cell. [From Ref 12].	14
Figure 9.	Diagram of photovoltaic cell [From Ref 13]	15
Figure 10.	Basics of Power Electronics [From Ref 18]	17
Figure 11.	Power Converter Multi-Disciplines [From Ref 18]	17
Figure 12.	Buck Converter [After Ref 16]	18
Figure 13.	Voltage and current changes [From Ref 16]	18
Figure 14.	Buck Converter at Boundary [From Ref 16]	20
Figure 15.	Buck Converter - Discontinuous Conduction [From Ref 16]	21
Figure 16.	Output Voltage vs Current [From Ref 16]	22
Figure 17.	Boost Converter Circuit [From Ref 16]	23
Figure 18.	Voltage and current waveforms (Boost Converter) [From Ref 16]	23
Figure 19.	Schematic for buck-boost converter [From Ref 16]	24
Figure 20.	Waveforms for buck-boost converter [From Ref 16]	24
Figure 21.	Comparison of Voltage ratio [From Ref 16]	25
Figure 22.	CUK Converter [From Ref 16]	26
Figure 23.	CUK "ON-STATE" [From Ref 16]	26
Figure 24.	CUK "OFF-STATE" [From Ref 16]	26
Figure 25.	Buck-Boost Converter [From Ref 16]	28
Figure 26.	Replacing inductor by transformer [From Ref 16]	28
Figure 27.	Flyback converter re-configured [From Ref 16]	28
Figure 28.	Forward Converter [From Ref 16]	29
Figure 29.	Forward converter with tertiary winding [From Ref 16]	29
Figure 30.	Uni-Solar LM-3 Solar Module and Ultra-Life Polymer Battery [From Ref 25]	32
Figure 31.	LM-3 12V Test mA Comparison Graph showing the difference with the technology incorporated [From Ref 25]	35
Figure 32.	LM-3 12V Test mW Comparison Graph [From Ref 25]	35

Figure 33.	LM-3 12V Test mA and mW Combined Comparison Graph [From Ref 25]	36
Figure 34.	LM-3 Variable Fixed Load Test Graphics [From Ref 25].....	38
Figure 35.	AN/PRC-119F (SINCGARS) [From Ref 19]	44
Figure 36.	AN/PSC-5 Tactical Satellite Telephone/Radio [From Ref 19].....	45
Figure 37.	AN/PRC-117F Secure Tactical Radio [From Ref 19]	45
Figure 38.	AN/PRC-150 VHF Radio [From Ref 19]	45
Figure 39.	Chemical Sensor [From Ref 19]	46
Figure 40.	Laser Target Identifier [From Ref 19]	46
Figure 41.	Laser/Rangefinder [From Ref 19].....	46
Figure 42.	M98A1 Javelin Missile System [From Ref 20]	47
Figure 43.	PP-8494 Battery Charger [From Ref 19]	47
Figure 44.	PP-8444 Battery Charger [From Ref 19]	48
Figure 45.	PVPCT System Prototype With Flexible Solar Array Deployed [From Ref 20]	48
Figure 46.	Alan Cocconi with SoLong at El Mirage Dry Lake in California. [From www.acpropulsion.com/ACP_PDFs/ACP_SoLong_Solar_UAV_2005-06-05.pdf]. Last accessed September 2005.....	49
Figure 47.	Global Hawk [from Ref 22].....	51
Figure 48.	Categories of UAV [From Ref 22]	52
Figure 49.	Computer generated model of NPSAT1. Note the three “rings” of solar arrays [From Ref 30].....	56
Figure 50.	NPSAT1 expanded view of Payload and Subsystems [From Ref 30].....	57
Figure 51.	NPSAT1 Solar Cell Array – Early Stage with Silicon Cells [From Ref 32] ...	58
Figure 52.	Middle Ring Solar Cell Array Layout [From Ref 1]	59
Figure 53.	Lithium-Ion Batteries Charge/Discharge Chart [From Ref 33]	60
Figure 54.	Improved Triple Junction Solar Cell I-V Curve [From Ref 34]	62
Figure 55.	Simplified cross-sectional view of Improved Triple Junction Solar Cell Layers [From Ref 34].....	63
Figure 56.	SPECTROLAB Improved Junction Solar Cells [From Ref 34]	63
Figure 57.	Some of the solar cell panels for NPSAT1, populated with Spectrolab ITJ cells (photo courtesy of Spectrolab).	64
Figure 58.	<i>I-V</i> curves of an ITJ cell for various incidence angles, taken by CDB, cell at 28°C [From Ref 1]	64
Figure 59.	<i>I-V</i> Characteristic Curve showing the Low Light Effect on Battery Charging. (From www.solengy.com/pages/whitepapers.html , July 2005).....	67
Figure 60.	Optimal Charging Window [From Ref 24].....	68
Figure 61.	Power Conversion Schematic [From Ref 24]	69
Figure 62.	Digital Photograph of the Photovoltaic Power Converter [From Ref 25]	69

LIST OF TABLES

Table 1.	Energy bandgap for typical semiconductors. The unit “eV” is electron-Volts, a common unit for describing electron energy (after Ref 7).....	6
Table 2.	LM-3 12V Test Descriptive Statistics [From Ref 25]	32
Table 3.	LM3 12V Test PVPC Charging Interval. Test Data at sunrise to sunset showing the difference with the technology incorporated [From Ref 25].....	34
Table 4.	LM-3 w/ Programmable Fixed Load Test Descriptive Statistics [From Ref 25]	37
Table 5.	LM-3 Flex Test w/ Programmable Fixed Load Excerpt [From Ref 25].....	37
Table 6.	Platoon Electronic Equipment and Battery Usage 5 day mission analysis. Source from Natick “Objective Force Warrior Program”	40
Table 7.	Platoon 5 day Battery analysis in Watt/Hours. Source from Natick “Objective Force Warrior Program”	41
Table 8.	Platoon 5 day Battery analysis in weight. Source from Natick “Objective Force Warrior Program”	42
Table 9.	Platoon 5-day battery analysis in dollars. Source from Natick “Objective Force Warrior Program”	43
Table 10.	UAV Capabilities [From Ref 22].....	52
Table 11.	Categories of UAV [From ref 22].....	53
Table 12.	Lithium-Ion Battery Data Table [From Ref 33]	61
Table 13.	Improved Triple Junction Solar Cells Electrical Parameters [From Ref 34]...	62
Table 14.	Estimated NPSAT1 Power Budget Requirement [From Ref 28]	66

THIS PAGE INTENTIONALLY LEFT BLANK

ACKNOWLEDGMENTS

The author wishes to thank everyone who contributed to the accomplishment of this work. First, I wish to express my utmost gratitude to my wife, my kids, and my parents for understanding and supporting me through the years of long hours, days, weeks, and even months of separation starting from my sea duty up to my time here at NPS.

I also like to thank Professor Sherif Michael for his guidance, support, contribution, and especially giving me the opportunity to work on this thesis. Many thanks are also in order to Professor Robert Ashton and Andrew Parker for their insights and guidance in improving this work. Their encouragements and contributions to my education have earned my utmost respect for their expertise and wisdom!

THIS PAGE INTENTIONALLY LEFT BLANK

EXECUTIVE SUMMARY

The abundance of solar energy from the sun has provided an alternative way to harness power that can be used for commercial, military and space applications. The purpose of this thesis is to consider Photovoltaic Power Converter (PVPC) technology, developed by Atira Technologies®, and its potential for military and space application. The research will confirm that PVPC technology enables a solar power system to produce usable power compared to the standard solar power system during low- and no-light conditions.

The resulting output power of a standard solar system varies depending on the illumination angle as well as the light intensity of each panel. The current technology for charging a battery to provide power is not efficient enough for full-scale implementation due to variations in lighting conditions. PhotoVoltaic (PV) cells are typically aligned in parallel and/or series in order to achieve higher current and potential respectively from the sunlight. For example, if a shadow is cast on one of the cells connected in series so that it is operating in a low-light condition, the cell basically stops contributing and limits the flow of the current in other cells. Those are some of the factors that affect the ability of photovoltaic cells to provide adequate power for different types of applications.

PVPC technology uses a converter that is specifically designed and useful for PV maximum power tracking purposes. The objective is to collect the maximum possible power from solar panels at all times, regardless of the load. The buck-boost converter is used because it makes it possible to efficiently convert a Direct Current (DC) voltage to either a lower or higher voltage. This switching topology would result in significant increase in the overall available power even in a subdued lighting condition. Although a small amount of power is generated, given enough time, a battery will reach its full charge, compared to no additional charging if the battery is using a solar panel without the PVPC circuit. A side by side comparison of the PVPC system and standard system during the tests show this vast improvement in power output over the standard solar power system.

The military uses a lot of equipment that runs on batteries. The ability to have uninterrupted communications and use of their equipment from an available power source is critical for their survival. In the field, military personnel can only carry a reasonable amount of weight to stay mobile. A battery charger is too heavy to carry around and only limited number of replacement batteries can be packed. PVPC technology will allow a more self-sufficient and mobile soldier. They would be less reliant on supply chains, carrying a smaller combat load due to elimination of unnecessary non-rechargeable batteries to power their equipment. Military intelligence can make or break the outcome of a mission or a war, therefore by incorporating PVPC technology into the current development in aviation we can have an unlimited supply of information on any area of interest. This is especially true with the very promising SoLong aircraft or other UAV prototype. The capability of charging various batteries using a single panel also exists with the use of this technology. Other military applications can benefit substantially from this new technology as proven from the test results.

As NPSAT1 is readied for launch to perform its various important missions, many technologies can be utilized or improved upon to enhance mission success. As seen from the test results, this converter circuit will be able to provide extra power to complement the main power source, supporting all the missions the satellite is intended to perform onboard NPSAT1. In addition, this back-up power source can provide up to 12 VDC, rated at 80W continuous and 150W peak. The converter utilizes switch-mode technology along with proven simple conversion and control technology in its circuitry in order to minimize maintenance and repair. Overall, with the back-up power source, the system power efficiency on board NPSAT1 can be expected to improve up to 20% compared to the current NPSAT1 power system. Obviously, this would allow for longer time on orbit for the satellite so it could extend its missions.

It became apparent that all tests conducted have shown that the PVPC produced more power than the standard system without the technology. Also, the fact that it was able to convert what was previously unusable power into usable power is a significant capability improvement by itself to the current technology for battery charging. In short,

PVPC's ability to provide more power can make a significant impact in the way our military conducts current and future missions.

THIS PAGE INTENTIONALLY LEFT BLANK

I. INTRODUCTION

A. BACKGROUND

Photovoltaic (PV) power conversion technology has been around for many years. Solar power systems have been implemented for military, space, commercial and residential applications by taking advantage of the abundant solar energy given off by the sun. Even with current technology, solar power systems are still not efficient enough for a full-scale implementation to provide power to battery chargers, motors, utility lines, computers, various equipment, etc. This is due to the standard solar power system's inability to produce usable power during subdued lighting conditions.

A company called Atira Technologies® has built a converter that uses PV power conversion technology which has potential for military and space use. The technology employed in this converter is basically a device that converts the power produced by a PV panel to a DC electrical current that charges a battery, which will then be used as either the primary or backup power source.

B. RESEARCH OBJECTIVES

This research attempts to verify the capability of a new kind of power converter which can be used for both military and space application. It is desired to see not only if the PV panels would work in low-light conditions, but whether the cells would work in no light conditions as well with the use of Atira's power converter, and finally, to consider the possibility of its usefulness and cost-effectiveness in today's field and space technology.

With the anticipated launching of NPSAT1 in the fall of 2006, the second objective of this research is to determine whether this charging circuit is feasible to be used on the satellite, thus improving available power to charge the spacecraft batteries.

C. RESEARCH QUESTIONS

1. Primary Research Question

In addition to improved efficiency, reliability, and cost-effectiveness, what are other aspects of this circuit design that will benefit the military in low wattage applications such as night vision devices, notebook computers, GPS units, and communication suites?

2. Secondary Research Questions

In addition to military applications, what are the potential benefits that this circuit would generate if employed in space applications, such as the NPSAT1 satellite?

D. SCOPE AND ORGANIZATION

The scope and organization of this project will include:

- A brief history and basic fundamental of photovoltaic solar energy technology
- A brief overview of basic power converters
- The analysis data gathered during the testing of the solar panels with and without the PVPC circuit
- A look into the military application of this improved circuitry
- Feasibility of switch-mode back-up power source for NPSAT1
- Conclusion of how the technology will benefit both the military and space application
- Recommendations for further/future research

E. METHODOLOGY

The research methodology for this project will consist of:

- A wide-ranging literature search of websites, publications, theses on systems research, and internet based materials.
- Analysis of the development, applications, tests and evaluations for the PVPC.

F. EXPECTED BENEFITS

This research will offer an apparent understanding of the capabilities of Photovoltaic Power Converting Technology (PVPC) and its stage of technological advancement. One of the many applications to which this may offer technology a solution is the area of field batteries. A reliable rechargeable battery system would lessen both the strategic burden and tactical load of fielded military personnel. This can be accomplished by reducing the reliance on disposable batteries in a forward deployed environment. Logistically and financially this change would make sense. In addition, its ability to improve the efficiency of the solar power output, cost-effectiveness, reliability, light weight, and unlimited power provide an invaluable benefit to the current level of technology for space application.

II. BASIC FUNDAMENTAL OF PHOTOVOLTAIC

The term photovoltaic (PV) refers to devices in which slivers of cells convert the solar energy falling on them directly into electricity. This occurrence is also known as photovoltaic effect. There are numerous applications of photovoltaics, such as power generation in a large scale, whether on house rooftops or in sizeable fields directly connected to the utility grid that provide clean, safe, and strategically sound alternatives to current methods of generating electricity. These solar cells convert the sun's energy into high quality electrical energy. Other photovoltaic cells such as thermo photovoltaic (TPV) cells convert infrared rays into electrical energy.

The underlying principle of solar cells is offered early on to enable understanding of the rest of this research. The energy from the sun, the solar cells' basic operation, and some of the characteristics of solar cell performance are presented in this chapter. All pertinent topics are discussed, but all properties of photovoltaics are not presented to limit going too much into unnecessary details about photovoltaic devices. Some good textbooks on semiconductor and photovoltaic physics can be referred to for more details, such as Reference [2].

Familiarity with semiconductors (p-n junctions) is assumed to fully understand this chapter. Furthermore, the understanding of the basic operation of diodes is also essential in the basic operation of solar cells.

A. SOLAR CONSTANT, IRRADIANCE, AND AIR MASS NUMBER

It is imperative to talk about the sun and the energy it provides before we discuss the process of solar cells' operation. After all, that is the source of electrical energy for the solar cells.

As the sun continuously delivers radiation with its entrained energy to us, it is the perfect steady-state emitter, called blackbody or a full radiator, whose spectrum can be approximated by a 6050K blackbody [2]. The spectrum can vary due to different temperatures across the sun. Therefore, the energy being provided by the sun or other radiant power source can be described by its irradiance. Irradiance is defined as the radiant power incident per unit area on a surface, usually measured in Watts per square

meter [1]. The irradiance of the sun in space just outside of the atmosphere is about $1.353 \text{ kW} / \text{m}^2$ [2, 3]. Since this number is so frequently used, it is also known as the solar constant (S_o). Due to seasonal changes, the solar constant will vary since the earth-sun distance varies as well. This variation is minimal to about only 3% [2].

It is also important to understand the air mass number for the performance of solar cells. This air mass number is completely different from the “air mass” associated with meteorology. It is an optical air mass in the solar spectrum.

The air mass number is defined as the path length through the atmosphere relative to the shortest path [2]. For instance, the shortest path from the space atmosphere to the earth’s surface is defined to have an air mass number of one. This is also defined and represented as AM1.

For a path length at a zenith angle z , the air mass number AM is defined in [2] to be

$$AM = \sec z \quad (2.1)$$

On the other hand, air mass number can also be expected by the shadow length s shed by a vertical structure of height l and calculating (given in [5])

$$AM = \sqrt{1 + \left(\frac{s}{l}\right)^2} \quad (2.2)$$

The figure below shows the relationship between the sun zenith angle and air mass number [4]. As the angle is increased, the path for sunlight increases, the air mass number increases, and the intensity of the solar spectrum decreases [1]. The air mass numbers can often describe the entire solar spectrum for a precise position. Similarly, the solar spectrum in outer space is defined as zero or AM0. Other AM numbers are used in terrestrial solar cell applications which will be discussed later in this chapter.

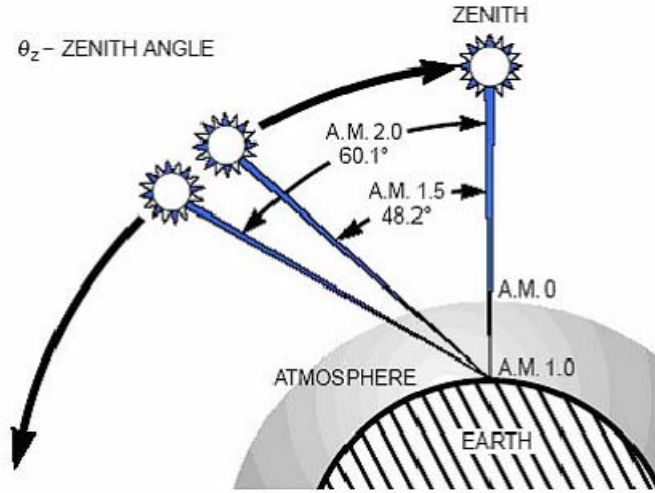


Figure 1. Illustration of the air mass number, path lengths, and zenith angles [From Ref 4].

B. SOLAR CELLS

1. Light Absorption and Material Selection

Photons are a type of electromagnetic (EM) radiation which contains specific amounts of energy. They differ in energy due to the different portions of the EM spectrum. This energy E_p is associated to its frequency by [1]

$$E_p = hf \quad (2.3)$$

where h is Planck's constant and f is the frequency of an EM field in Hertz (Hz) [6].

Consequently, for each frequency there is a corresponding energy in the EM spectrum. The wavelength and speed of propagation are also related to frequency; so, the photon energy can be expressed by [1]

$$E_p = \frac{hc}{\lambda} \quad (2.4)$$

where c is the speed of light and λ is the electromagnetic wavelength [6]. All photons have the same amount of energy in them at any specific wavelength or frequency, no matter what the strength of the field or the brightness of the light. The amount of photons acting on a surface area per unit time provides the intensity.

All semiconductors have energy bandgap E_g . Energies greater than the bandgap are required to move an electron in the valence band to the conduction band. This result can be achieved by photons with enough energy. Therefore, E_p should be greater than E_g for the semiconductor to absorb photons. When this happens, an electron is excited to the conduction band. Each photon will generate only one electron-hole pair; any excess energy is dissipated as heat [6]. For photons containing less energy than the bandgap, they will just pass through the semiconductor and never produce any electron-hole pairs. As a result, only a semiconductor with suitable energy bandgap is used to be able to absorb the sun's light. This is important to take advantage of the solar spectrum. As an example, if a silicon cell has a bandgap of 1.11 eV ($1\text{eV} = 1.6 \times 10^{-19} \text{J}$) and using Equation (2.4), and assuming the speed of light in a vacuum, the maximum wavelength it can absorb is 1.1 μm . Most of the photons that can be absorbed are in the visible spectrum. It's one of the reasons why silicon was chosen for solar cells. Table 1 lists all the typical energy bandgaps for semiconductors [7].

Other materials are also used for solar cells. Some of the advanced solar cells are made of multi-layered materials which absorb many photons resulting in a wider range of wavelengths. More recent research allows the use of photovoltaic cells that convert source energy from other spectra into electrical energy, such as thermo photovoltaic cells (absorbing heat, or infrared rays) [8]. The same idea is used; where the material used is specifically selected to absorb the preferred wavelengths.

Table 1. Energy bandgap for typical semiconductors. The unit "eV" is electron-Volts, a common unit for describing electron energy (after Ref 7).

Material	Symbol	Bandgap (eV)
Diamond	C	5.5
Silicon	Si	1.11
Germanium	Ge	0.67
Gallium Phosphide	GaP	2.26
Gallium Arsenide	GaAs	1.43
Indium Phosphide	InP	1.34
Indium Antimonide	InSb	0.18

2. Generation of Current

External current cannot be created by a diode alone. Drift and diffusion currents which are internal to the system are undetectable outside of the diode. Nevertheless, some energy source will create excitation of electrons and the excess free electrons will want to flow and create current. Also, this excitation generates electron-hole pairs. Electrons freed in the n side will be repelled by the electric field, forcing them away from the depletion region. They will gather at the cathode (the n terminal). The holes will be swept by the electric field to the p side, resulting in excess holes in the p side, gathered at the anode (the p terminal). If the anode and the cathode of the $p-n$ junction are connected together through a conductor (short circuit), the excess electrons at the cathode will want to follow the wire toward the anode. The holes will go in the opposite direction from the anode to the cathode, consequently resulting in an external current flow. Because of current direction convention, the direction of current for the solar cell is out of the anode and into the cathode. This current is called the short-circuit current, I_{sc} [6]. Also, note that current direction is opposite of that of the solar cell.

Again, photons generating the electron excitation in a solar cell with sufficient energy will create electron-hole pairs, thus allowing the current generation to occur or current I_{sc} generated when the cell is illuminated. High temperature will also cause thermal excitation, but the amount is small compared to photon excitation [6].

3. Solar Cells Characterization

All solar cells can be characterized by their current-voltage curve, or $I-V$ curve, and the following properties that describe the cell's performance [2]:

I_{sc}	Short-circuit current
V_{oc}	Open-circuit voltage
P_{MAX}	Maximum output power
η	Conversion efficiency
ff	Fill factor – “square ness” of the curve

A plot of output current against the output voltage of the solar cell is called the $I-V$ curve when it is under illumination. This plot is the same as that of a diode. For a regular diode, the current-voltage relationship is given by [1]

$$I = I_o (e^{V/nV_T} - 1) \quad (2.5)$$

where I_o is the saturation current that is a property of the diode, n is a constant dependent on the diode material, and V_T is the thermal voltage [9]. If a solar cell is not getting any light, its current-voltage relationship is given by Equation (2.5). Clearly, the cell will generate its own current when illuminated. At zero voltage (short-circuit), the current generated is simply I_{SC} [5]. Then for an illuminated solar cell, the ideal $I-V$ relationship is [1]

$$I = I_o (e^{V/nV_T} - 1) - I_{SC} \quad (2.6)$$

The result is the $I-V$ curve of the diode translated downward by I_{SC} [19]. The short circuit current is subtracted because it is flowing in the opposite direction of the regular diode. A basic plot of the dark and illuminated $I-V$ curves using Equations (2.5) and (2.6) is shown in the figure below [5]. The illuminated $I-V$ curve is in the fourth quadrant of the $I-V$ plane, indicating that power is being supplied to the load [8].

In general, solar cells' $I-V$ curves are plotted with voltage reflected about the x-axis so that the current is considered positive [5]. Similarly, Figure 3 shows the same in order that I_{SC} is positive as shown in the manufacturer's specification sheets.

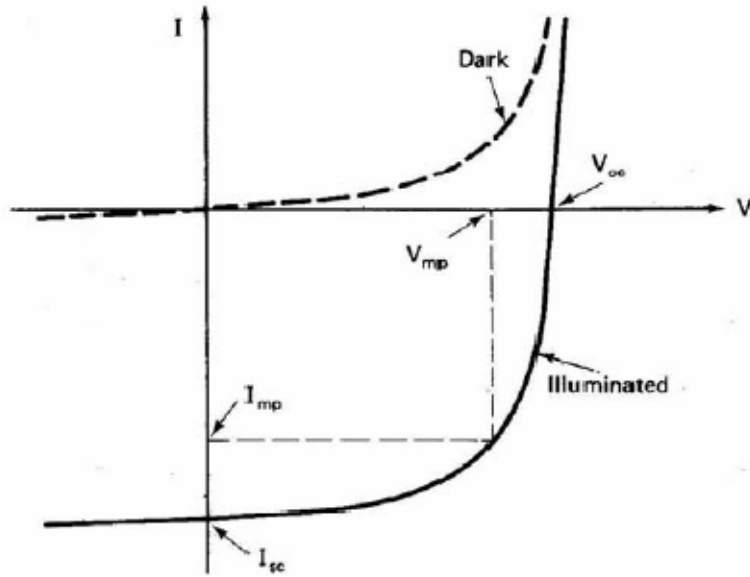


Figure 2. Output current-voltage relationship for a $p-n$ junction when dark and illuminated [After Ref 5].

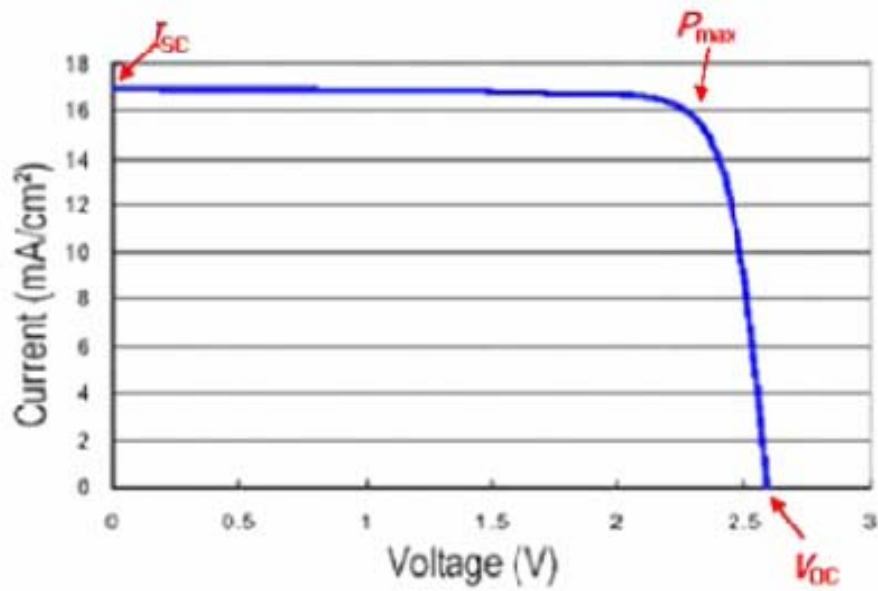


Figure 3. A sample $I-V$ curve for a solar cell with properties marked. In this example, the curve is for a triple-junction solar cell [After Ref 23].

The *open-circuit voltage* is the voltage across the cell when the output current is zero [5]. And so, set I to zero using Equation (2.6) to find the open-circuit voltage V_{OC} to obtain [1]

$$V_{OC} = nV_T \ln\left(\frac{I_{SC}}{I_o} + 1\right) \quad (2.7)$$

For that reason, the solar cell's open-circuit voltage relies on short-circuit current.

The cell output power is found by $P = IV$, and there is a point (V_{mp}, I_{mp}) that will maximize the output power [5], resulting in [1]

$$P_{MAX} = I_{mp} V_{mp}. \quad (2.8)$$

Equation (2.8) is the maximum power delivered by the solar cell. Normally, loads are adjusted accordingly for the cell to operate close to the maximum power point.

The efficiency of energy conversion varies on the input power to the solar cell. Remember that for AM0, the input power would be the solar constant (1.353 kW/m²). Letting C be the solar constant and A be the area of the receiving surface in square meters, the efficiency η , given in [5], is [1]

$$\eta = \frac{P_{\max}}{P_{in}} = \frac{P_{\max}}{AC} \quad (2.9)$$

The last but not the least of the properties is the fill factor, ff , found by [1]

$$ff = \frac{P_{\max}}{V_{oc} I_{sc}} \quad (2.10)$$

The fill factor is a measure of how “square” the curve is [5]. Typically, the fill factor will be between 0.7 and 0.85 [5].

Finally, a common circuit symbol for the solar cell is a diode symbol with a circle around it, and with arrows pointing toward the diode/circle to indicate light shining on the cell, as shown in Figure 4 [1]. Whereas for a diode the current goes into the “fat” end of the arrow (the anode) and comes out of the arrowhead (the cathode), the solar cell's current direction is the opposite [10].

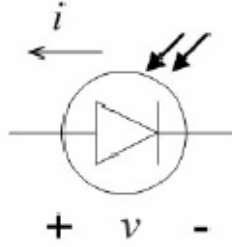


Figure 4. Circuit symbol for the solar cell. Note the current direction [From Ref 10].

4. Factors Affecting the Solar Cell Output

There are many factors that affect solar cell's performance such as radiation, temperature, light incidence angle, series and parallel resistance, etc. [5]. The effect of light incidence angle and temperature will be examined for the purpose of this thesis.

Maximum output from the cell is achieved if the incident light is directly perpendicular to the surface of the solar cell. This output current will gradually decrease as the incidence angle deviates from the ideal condition. The new value of the short-circuit current, with a light incidence angle θ from the normal (i.e., the angle between the incident light ray and the normal to the cell surface), is $I_{sc} \cos \theta$ [10]. On the other hand, the open-circuit voltage does not decrease significantly for large angles deviated from the ideal since it is not strongly dependent on the amount of light received.

As the angle from the normal approaches 60° and above, the current becomes less than the predicted value of $0.5I_{sc}$. This is due to optical refraction and reflection at the surface of the cell, whose effects become important at large angles [1].

The effect of temperature on solar cells' operation in space is very important due to consistent changes in temperature in space. Even though the short-circuit current is not strongly affected by temperature, it does increase slightly with increasing temperature [5]. However, the open-circuit voltage is more susceptible to temperature changes.

M.A. Green [5] gives an expression for the variation in voltage with respect to temperature. The expression given in [5], stated here without proof, is [1]

$$\frac{dV_{oc}}{dT} = -\frac{(E_{g0}/q) - V_{oc} + \gamma V_T}{T} \quad (2.11)$$

where E_{g0} is the “linearly extrapolated zero temperature bandgap of the semiconductor” making up the cell, V_T is the thermal voltage, and γ includes the temperature dependencies of the parameters determining I_o of the cell. Equation (2.11) states that the voltage decreases linearly with temperature. Substituting values for silicon (given in [5] as $E_{g0}/q \sim 1.2$ V, $V_{oc} \sim 0.6$ V, $\gamma \sim 3$, $T = 300$ K) gives [1]

$$\frac{dV_{oc}}{dT} = -\frac{1.2 - 0.6 + 0.078}{300} = -2.3 \text{ mV}/^\circ\text{C}. \quad (2.12)$$

For this reason, for every degree increase of temperature in Celsius or Kelvin, the open – circuit voltage can decrease 2.3 mV as shown in Figure 5.

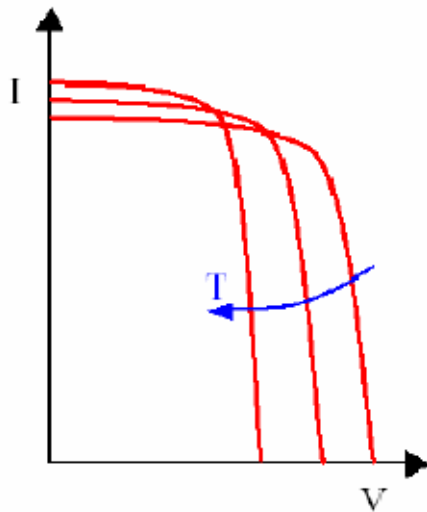


Figure 5. The effect of temperature on the solar cell's output. Increasing temperature will decrease the open-circuit voltage, while slightly raising the short circuit current [From Ref 11].

The effect of temperature is greater on multi-junction solar cells. A good estimate is to predict a -2 mV/ $^\circ\text{C}$ change for each $p-n$ junction [10]. For a triple-junction solar cell, discussed in the next section, there are three $p-n$ junctions. Therefore, the triple-junction cell's open-circuit voltage is dependent on temperature by about -6 mV/ $^\circ\text{C}$ [1].

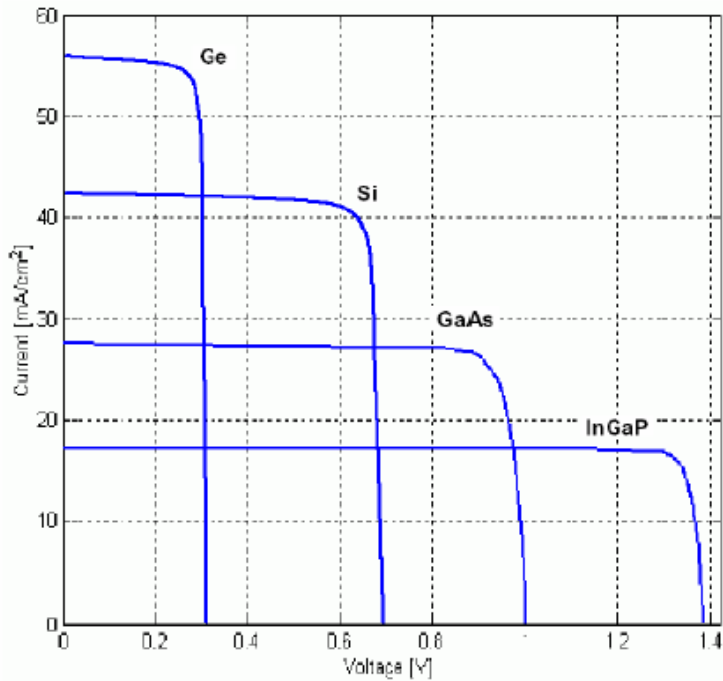


Figure 6. Typical I - V curves for the various single-junction cell technologies [From Ref 11].

5. Multi-Junction Solar Cells

Using multiple layers of different material which are stacked together can improve the efficiency of photon absorption. Multi-junction cells are available in two or three junctions. Two $p-n$ junctions are stacked on top of each other to create dual-junction (DJ) solar cells. Evidently, triple junction solar cells are three $p-n$ stacked together. Layers consist of different materials to absorb photons in a wide range of wavelengths. Spectrolab provided a detailed diagram of a common TJ cells that are made of GaInP₂/GaAs/Ge layers as shown in the figure below. The GaInP₂ (higher bandgap) are located on top and Germanium was placed on the bottom [27]. The higher energy photons will be absorbed by the higher bandgap material and lower energy photons will be absorbed by the lower layers. This allows the cell to absorb more photons, thus providing better efficiency than single junction cells.

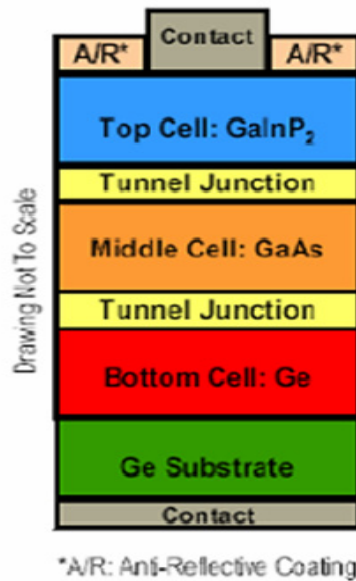


Figure 7. Simplified cross-sectional view of Improved Triple Junction Solar Cell Layers [From Ref 27]

C. TERRESTRIAL AND SPACE SOLAR CELLS

As stated in the above discussion, solar cells convert solar energy to electrical energy. Current is created by the movement of electrons using the photons in sunlight to provide the energy that moves electrons from one layer of a semi-conducting metallic wafer to another.

Two of the most common use solar cells today are silicon and gallium arsenide which come in several different grades and varying efficiencies. Gallium arsenide is used in orbiting satellites while silicon is more commonly used for Earth-based (terrestrial) applications. Figure 8 below shows a cut-away detailed photo of a PV solar cell.

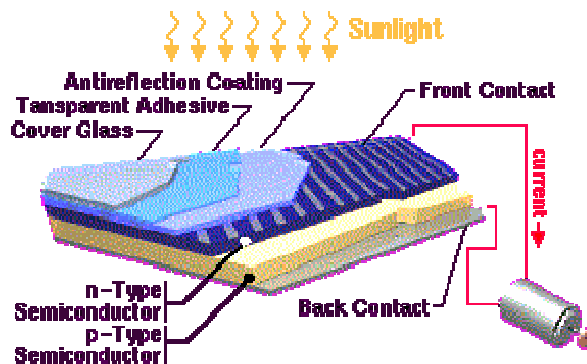


Figure 8. A Photovoltaic solar cell. [From Ref 12]

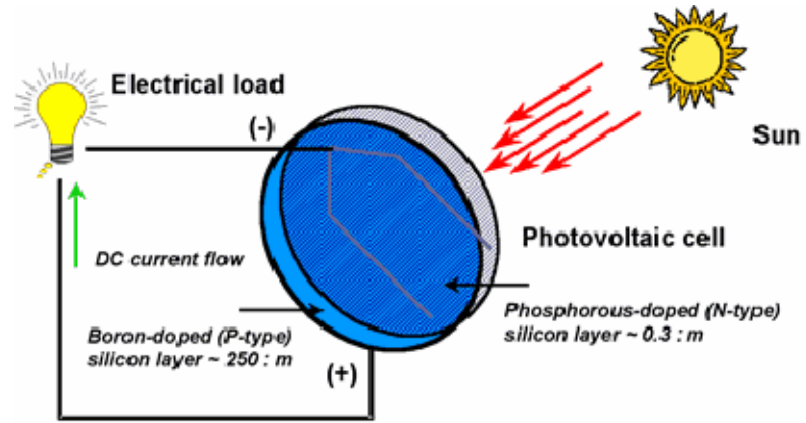


Figure 9. Diagram of photovoltaic cell [From Ref 13]

THIS PAGE INTENTIONALLY LEFT BLANK

III. BASIC PRINCIPLE OF POWER CONVERTERS

In this chapter, the basic background information and a brief summary of direct current to direct current (dc-dc) power converters is covered for the reader to gain the necessary understanding of the different kinds of power converter topologies. References such as References 15 and 17 provide a more in-depth look at different kinds of power converters.

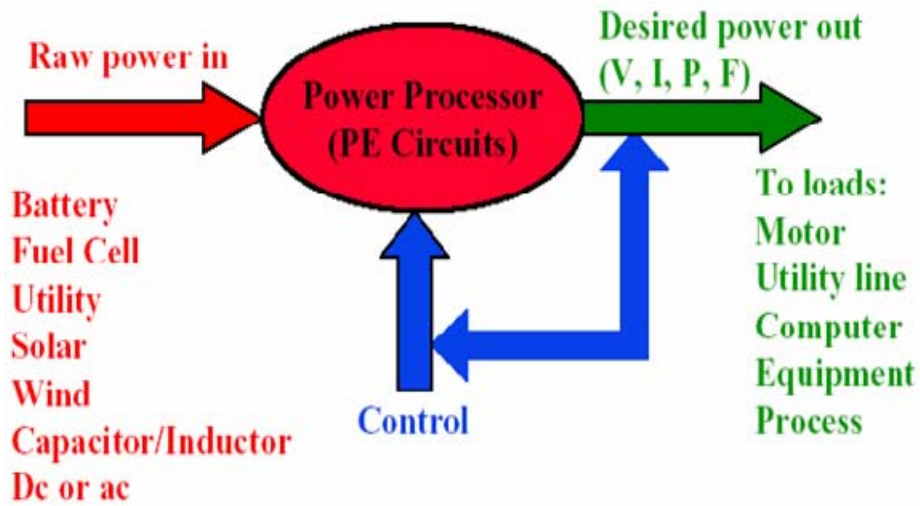


Figure 10. Basics of Power Electronics [From Ref 18]

Multi-disciplinary Nature of Power Electronics

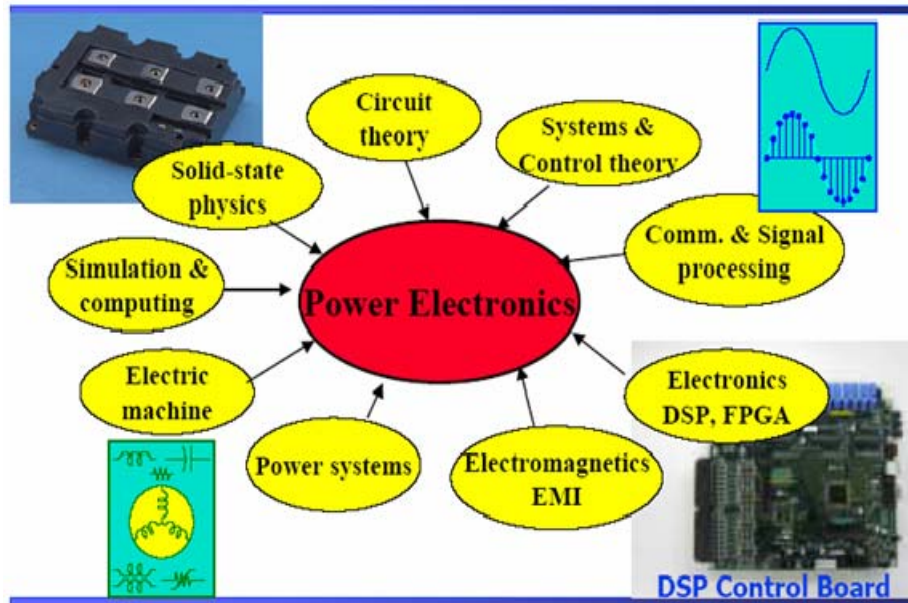


Figure 11. Power Converter Multi-Disciplines [From Ref 18]

A. DC-DC CONVERTER BASICS

A device that accepts a dc input voltage and produces a dc output voltage is called a dc-dc converter. In general, the dc output voltage is at a different voltage level than the input. Additionally, these types of converters can be used to provide noise isolation, power bus regulation, dc motor drives, etc. The following is a brief review of some of the most popular dc-dc converter topologies.

1. Buck Converter/Step-Down Converter

From the below diagram, the basic characteristic of the buck/step down converter is that the input V_{in} is greater than the output voltage V_o . The two modes of operation are continuous and discontinuous. When the transistor Q is gated “on”, the circuit is configured in continuous mode and the voltage drop $V_{in} - V_x$ becomes zero. The diode D is reverse biased and $V_x = V_{in}$. When the transistor Q is gated “off”, the circuit is configured in discontinuous mode. The current will still be flowing but through the diode and the voltage at V_x will just be equal to the voltage across the conducting diode during the full “off” time and $V_x = 0$. Assuming that the value of the capacitor (C) is very large and employed as a low-pass filter, the converter output voltage is essentially equal to the dc component $v_o(t) \approx V_o$.

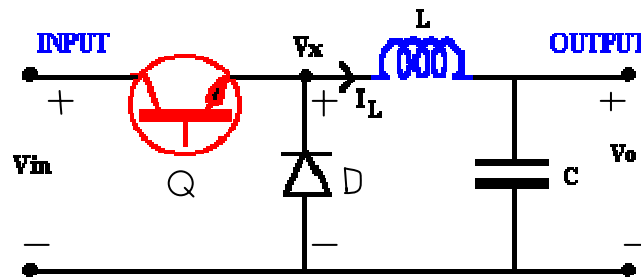


Figure 12. Buck Converter [After Ref 16]

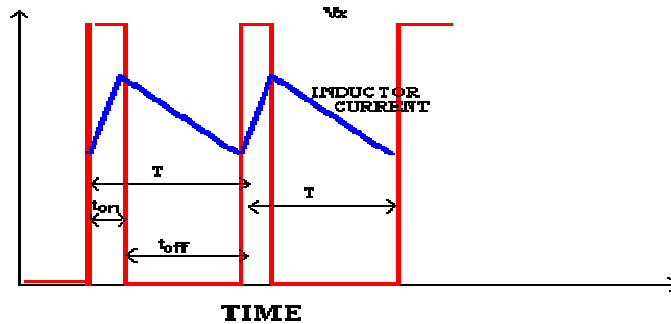


Figure 13. Voltage and current changes [From Ref 16]

Consider the changes in the inductor current over a cycle to be able to analyze the voltages from this circuit and from the relation shown in the equations below [16]

$$V_x - V_o = L \frac{di}{dt} \quad (3.1)$$

the change of current satisfies

$$di = \int_{ON} (V_x - V_o) dt + \int_{OFF} (V_x - V_o) dt \quad (3.2)$$

During a steady state operation, the current at the start and end of a period T will not change [16]. To get a simple relation between voltages we assume no voltage drop across transistor or diode while “on” and a perfect switch change. Thus during the “on” time $V_x = V_{in}$ and in the “off” $V_x = 0$. Thus, the equations below [16]

$$0 = di = \int_0^{t_{on}} (V_{in} - V_o) dt + \int_{t_{on}}^{t_{on}+t_{off}} (-V_o) dt \quad (3.3)$$

which simplifies to

$$(V_{in} - V_o)t_{on} - V_o t_{off} = 0 \quad (3.4)$$

or

$$\frac{V_o}{V_{in}} = \frac{t_{on}}{T} \quad (3.5)$$

and defining "duty ratio" as

$$D = \frac{t_{on}}{T} \quad (3.6)$$

the voltage relationship becomes $V_o = D * V_{in}$. Since the circuit is lossless and the input and output powers must match, on the average $V_o * I_o = V_{in} * I_{in}$. Thus the average input and output current must satisfy $I_{in} = D * I_o$. These relations are based on the assumption that the inductor current does not reach zero [16].

a. Transition Between Continuous and Discontinuous

When the current in the inductor L remains always positive then either the transistor $T1$ or the diode $D1$ must be conducting. For continuous conduction the voltage V_x is either V_{in} or 0. If the inductor current ever goes to zero then the output voltage will not be forced to either of these conditions. At this transition point the current just reaches zero as seen in Figure 14. During the “on” time $V_{in} - V_{out}$ is across the inductor thus the equation below [16]

$$I_L(\text{peak}) = (V_{in} - V_{out}) \cdot \frac{t_{on}}{L} \quad (3.7)$$

The average current which must match the output current satisfies

$$I_L(\text{average at transition}) = \frac{I_L(\text{peak})}{2} = (V_{in} - V_{out}) \frac{dT}{2L} = I_{out}(\text{transition}) \quad (3.8)$$

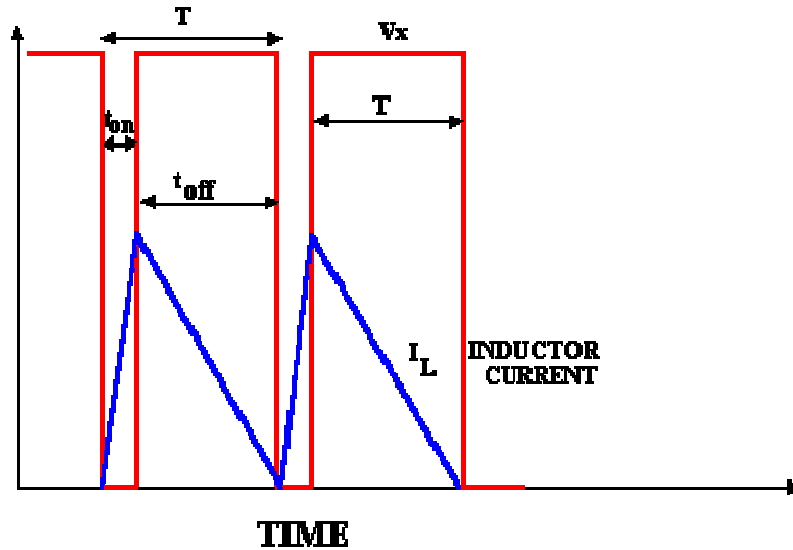


Figure 14. Buck Converter at Boundary [From Ref 16]

If the input voltage is constant the output current at the transition point satisfies [16]

$$I_{out}(\text{transition}) = V_{in} \frac{(1-d)d}{2L} T \quad (3.9)$$

b. Voltage Ratio of Buck Converter (Discontinuous Mode)

We can use the fact that the integral of voltage across the inductor is zero over a cycle of switching T for the continuous conduction analysis we use. Divide the

transistor “off” time into segments of diode conduction $d_d T$ and zero conduction $d_o T$. The inductor average voltage thus gives the equations below [16]

$$(V_{in} - V_o)DT + (-V_o)\delta_d T = 0 \quad (3.10)$$

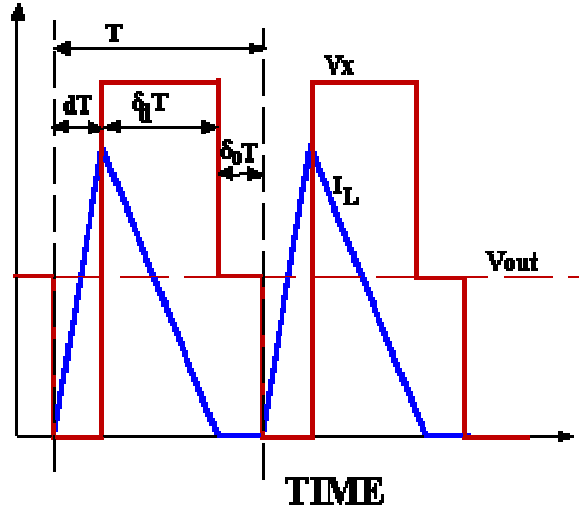


Figure 15. Buck Converter - Discontinuous Conduction [From Ref 16]

$$\therefore \frac{V_{out}}{V_{in}} = \frac{d}{d + \delta_d} \quad (3.11)$$

for the case $d + \delta_d < 1$. To resolve the value of δ_d consider the output current which is half the peak when averaged over the conduction times $d + \delta_d$

$$I_{out} = \frac{I_L(peak)}{2} (d + \delta_d) \quad (3.12)$$

Considering the change of current during the diode conduction time

$$I_L(peak) = \frac{V_o(\delta_d)}{L} \quad (3.13)$$

Thus from (3.12) and (3.13) we can get

$$I_{out} = \frac{V_o \delta_d T \cdot (d + \delta_d)}{2L} \quad (3.14)$$

using the relationship in (3.11)

$$I_{out} = \frac{V_{in} d \delta_d T}{2L} \quad (3.15)$$

and solving for the diode conduction

$$\delta_d = \frac{2 L I_{out}}{V_{in} d T} \quad (3.16)$$

The output voltage is thus given as

$$\frac{V_{out}}{V_{in}} = \frac{d^2}{d^2 + \left(\frac{2 L I_{out}}{V_{in} T}\right)} \quad (3.17)$$

defining $k^* = 2L/(V_{in}T)$, we can see the effect of discontinuous current on the voltage ratio of the converter.

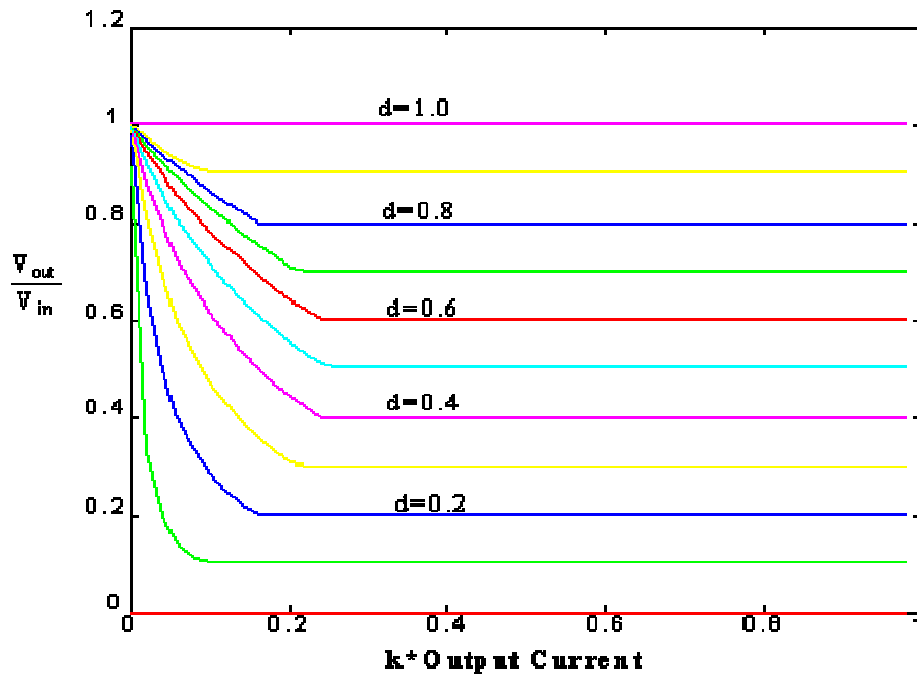


Figure 16. Output Voltage vs Current [From Ref 16]

The figure shows that when the output current is high enough, the voltage ratio depends only on the duty ratio "d". It increases the output voltage of the converter towards V_{in} during the discontinuous operation at low.

2. Boost Converter Step-Up Converter

The schematic shows the basic boost converter in Figure 17. When a higher output voltage than input is required this circuit is used.

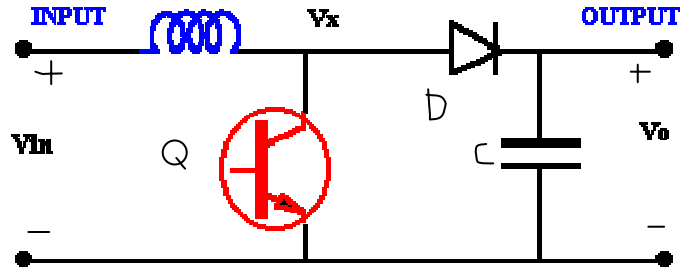


Figure 17. Boost Converter Circuit [From Ref 16]

When the transistor is “on”, $V_x = V_{in}$, and when it is “off” the inductor current flows through the diode giving $V_x = V_o$. It is assumed that the inductor current remains flowing (during continuous conduction) for this analysis. The voltage across the inductor is shown in Figure 18 and the average must be zero for the average current to remain in steady state given in the equations below [16]

$$V_{in}t_{on} = +(V_{in} - V_o)t_{off} = 0 \tag{3.18}$$

This can be rearranged as

$$\frac{V_o}{V_{in}} = \frac{T}{t_{off}} = \frac{1}{(1-D)} \tag{3.19}$$

and for a lossless circuit the power balance ensures

$$\frac{I_o}{I_{in}} = (1-D) \tag{3.20}$$

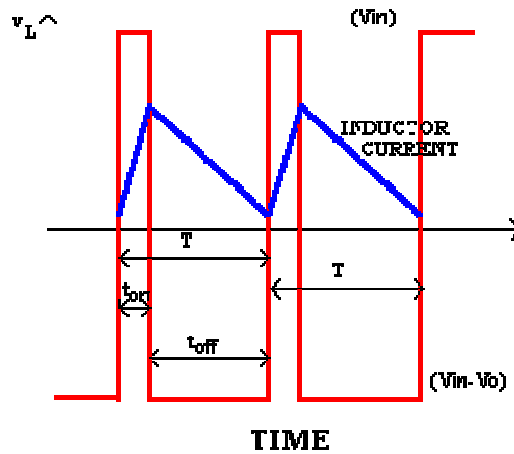


Figure 18. Voltage and current waveforms (Boost Converter) [From Ref 16]

The output voltage must always be greater than the input voltage in magnitude since the duty ratio "D" is always between 0 and 1. The negative sign indicates a reversal of sense of the output voltage [16].

3. Buck-Boost Converter

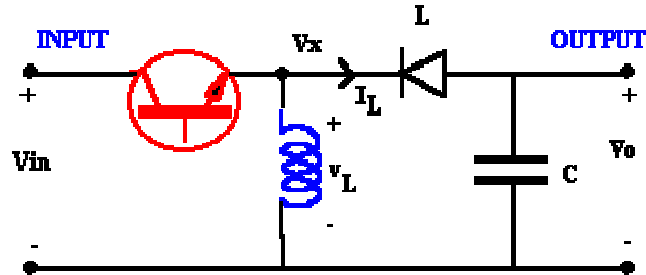


Figure 19. Schematic for buck-boost converter [From Ref 16]

Buck-boost converters make it possible to efficiently convert a dc voltage to either a lower or higher voltage. Buck-boost converters are especially useful for PV maximum power tracking purposes, where the objective is to draw maximum possible power from solar panels at all times, regardless of the load.

During the continuous conduction of the buck-boost converter $V_x = V_{in}$ when the transistor is “on” and $V_x = V_o$ when the transistor is “off”. For zero net current change over a period the average voltage across the inductor is zero in the equations below [16]

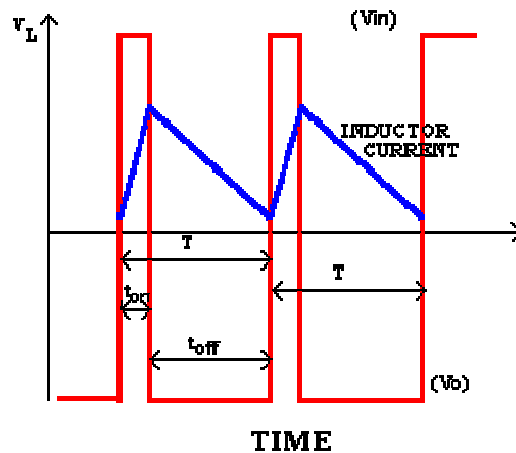


Figure 20. Waveforms for buck-boost converter [From Ref 16]

$$V_{in}t_{ON} + V_o t_{OFF} = 0 \quad (3.21)$$

which gives the voltage ratio

$$\frac{V_o}{V_{in}} = -\frac{D}{(1-D)} \quad (3.22)$$

and the corresponding current

$$\frac{I_o}{I_{in}} = -\frac{(1-D)}{D} \quad (3.23)$$

B. CONVERTER COMPARISON

Figure 21 shows the voltage ratios achievable by the dc-dc converters. A linear relationship between the control (duty ratio) and output voltage can be seen for the buck converter. For the buck-boost converter, it can either reduce or increase the voltage ratio with unit gain for a duty ratio of 50%.

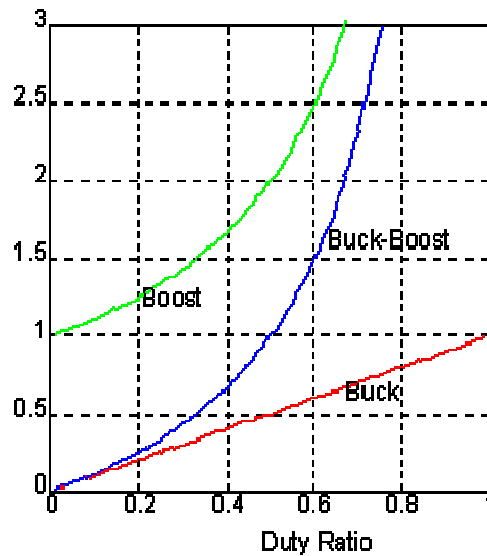


Figure 21. Comparison of Voltage ratio [From Ref 16]

C. OTHER CONVERTERS

1. Cuk Converter

The analysis for the Cuk converter is based on the voltage balance across the inductor. For the buck, boost and buck-boost converters, emphasis is on the transferred

energy between inputs and output using the inductor. The Cuk converter uses capacitive energy transfer and analysis is based on current balance of the capacitor [16]. The circuit in Figure 22 is derived from duality principle on the buck-boost converter.

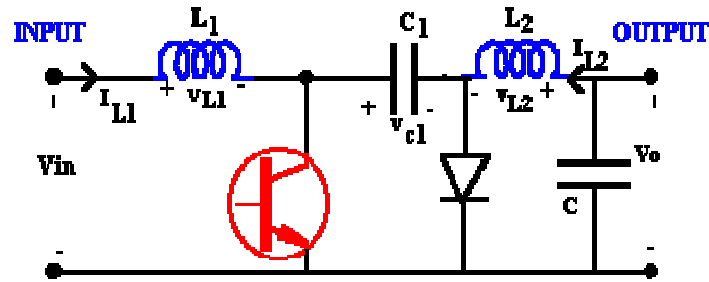


Figure 22. CUK Converter [From Ref 16]

We can examine the charge balance for the capacitor C_1 if we assume that the current through the inductors is essentially rippled free. For the transistor “on” the circuit becomes [16]

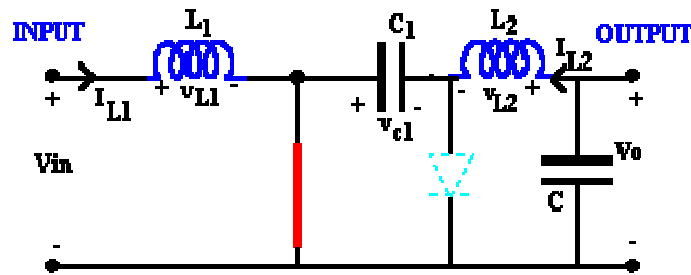


Figure 23. CUK "ON-STATE" [From Ref 16]

and the current in C_1 is I_{L1} . When the transistor is “off”, the diode conducts and the current in C_1 become I_{L2} .

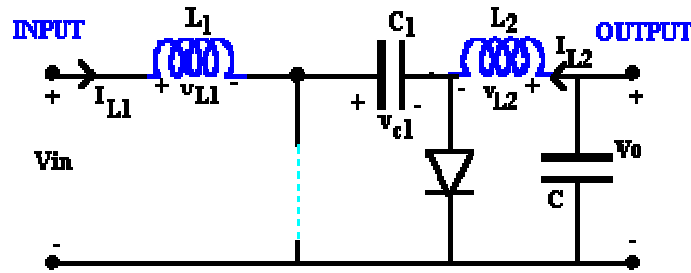


Figure 24. CUK "OFF-STATE" [From Ref 16]

Since the steady state assumes no net capacitor voltage rise, the net current is zero as shown in the following equation [16]

$$I_{L1}t_{ON} + (-I_{L2})t_{OFF} = 0 \quad (3.24)$$

which implies

$$\frac{*I_{L2}}{I_{L1}} = \frac{(1-D)}{D} \quad (3.25)$$

The inductor currents match the input and output currents, thus using the power conservation rule

$$\frac{V_o}{V_{in}} = -\frac{D}{(1-D)} \quad (3.26)$$

Thus the voltage ratio is the equal to the buck-boost converter. The input and output inductors create a smooth current at both sides of the Cuk converter. This is one of the advantages of this converter since the buck, boost and buck-boost have at least one side with pulsed current.

2. Isolated DC-DC Converters

Multiple outputs are required and output isolation may need to be implemented depending on the application. Additionally, some input-to-output isolation may be required to meet safety standards or provide impedance matching. Different dc-dc topologies covered earlier can be adapted to provide isolation between input and output.

3. Flyback Converter

The flyback converter is a derivation of the buck-boost converter. Figure 25 shows the basic buck-boost converter; and Figure 26 changes the inductor with a transformer. The buck-boost converter works by storing energy in the inductor during the “on” phase and releasing it to the output during the “off” phase [16]. By magnetization of the transformer core, the energy is stored in the process. A gapped core is often used to increase the stored energy.

Figure 27 depicts the isolated output is clarified by removal of the common reference of the input and output circuits.

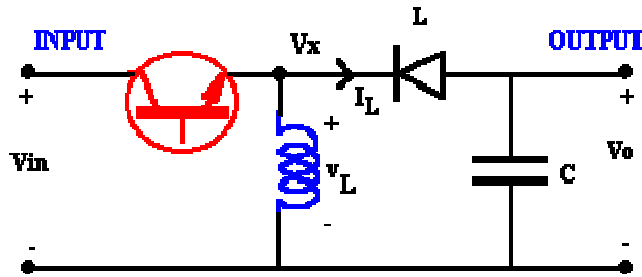


Figure 25. Buck-Boost Converter [From Ref 16]

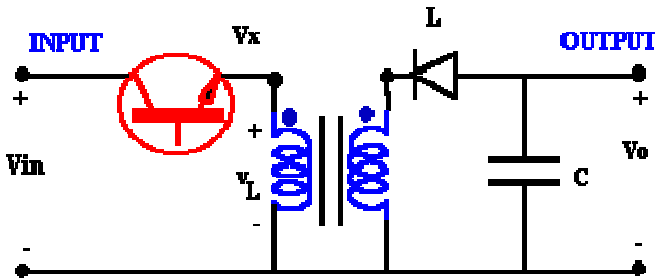


Figure 26. Replacing inductor by transformer [From Ref 16]

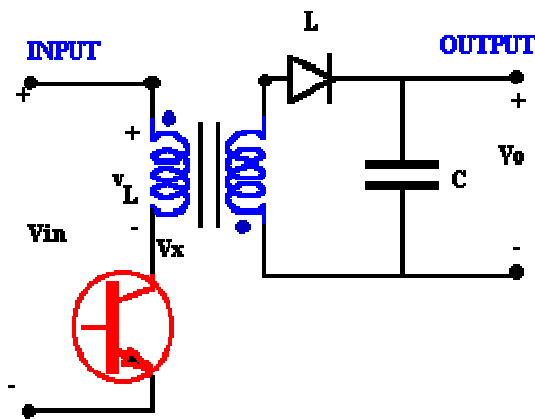


Figure 27. Flyback converter re-configured [From Ref 16]

4. Forward Converter

The way a forward converter functions is that of the ideal transformer converting the input AC voltage to an isolated secondary output voltage. When the transistor is “on”, V_{in} appears across the primary and then generates the equation below as shown in Figure 28 [16]

$$V_x = \frac{N_1}{N_2} V_{in} \quad (3.27)$$

To ensure only positive voltages are applied to the output circuit, diode D1 is used on the secondary while D2 provides a circulating path for inductor current if the transformer voltage is zero or negative.

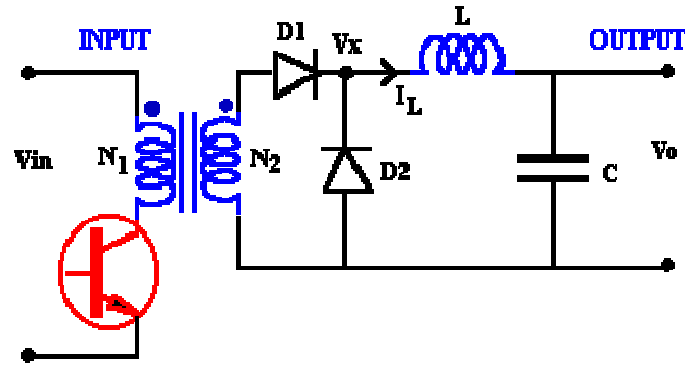


Figure 28. Forward Converter [From Ref 16]

In Figure 28, the problem with the operation of the circuit is that only positive voltage is applied across the core, thus flux can only increase with the application of the supply. The flux will continue to increase until the core is saturated, when the magnetizing current increases significantly and circuit failure occurs. When there is no significant dc component to the input voltage, the transformer can sustain operation. There is positive voltage across the core and the flux increases while the switch is “on”, and we need to supply negative voltage to reset the core flux when the switch turns “off”.

A tertiary winding with a diode connection to permit reverse current is shown in Figure 29. Take notice that the "dot" convention on the tertiary winding is opposite those of the other windings. The current was flowing in a "dot" terminal when the switch turns off. The core inductance act to continue current in a dotted terminal, thus

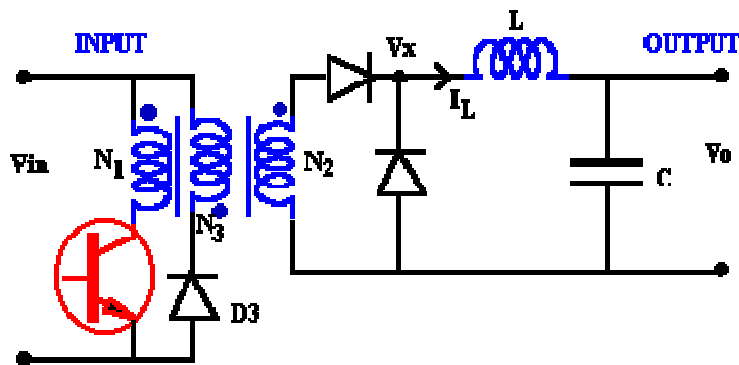


Figure 29. Forward converter with tertiary winding [From Ref 16]

THIS PAGE INTENTIONALLY LEFT BLANK

IV. DATA ANALYSIS

A. INTRODUCTION

This section of the paper will introduce the data analysis from the tests conducted using the PhotoVoltaic Power Converter (PVPC) technology by the team of Atira engineers and NPS students from both the engineering and business curricula. The tables and graphs below show the data collected for an experiment conducted on a clear day from sunrise to sunset on a typical day in February 2005.

Individual test data gathered during the research was used to present the validity of the PVPC technology. The documentations and factual data will allow us to decide whether or not a solar panel integrated with PVPC can generate more power than the one without it. We will first look at the tests performed by Atira, and then the tests conducted at NPS. Information from the test data was drawn out using standardized and automated analytical tools. A concise description for each test was explained with tables and graphical methods to render further clarity. We will then examine the result to support our complete evaluation and conclusion regarding the performance of the PVPC technology.

B. TEST ANALYSIS

A parallel comparison for the test approach was used to measure the performance levels of the solar panels with the PVPC technology and a system without it. For ease of identifying the power systems, the solar panel with the PVPC technology will be referred to as “PVPC Panel” and the solar panel without the PVPC technology will be referred to as “Typical Panel”. Two main data elements, current in Milli-ampere and power in Watts, will be looked at for measuring the amount of energy each system is generating. From each solar panel, the current is the main measurable output and against the voltage from the load source results in the power. We will use the power as the normal measurement to provide us with a consistent result from the tests that can have a variable input or load. A tabulated and graphical result was generated to easily allow us to recognize any considerable differences.

1. Uni-Solar LM-3 Test

Tests were done on Uni-Solar LM-3 module and UBC36106102/PCM Ultra-Life Polymer 3.7 V rechargeable batteries with the current and power output measured at frequent intervals using a 12 Volt battery. A 12V battery was needed to demonstrate the ability to enhance a usual solar power system; therefore, three Ultra-Life Polymer batteries were wired in series to act as 12V battery load. The generated power is lost or unusable if the system cannot convert enough solar power into electrical power to overcome the batteries' charging threshold. This leads us to the Uni-Solar LM-3 module designed to only charge a 9V battery and does not provide enough power to charge a 12V battery. By incorporating the PVPC to the module, it can significantly improve the output power to charge the 12V battery.

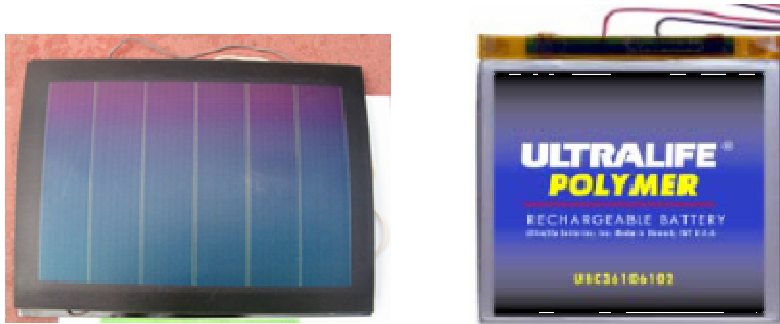


Figure 30. Uni-Solar LM-3 Solar Module and Ultra-Life Polymer Battery [From Ref 25]

Atira conducted the test from 0730 to 1730, a span of 10 hours, taking 18 data readings. The table below shows the result for the test on the PVPC panel and typical panel battery in current (mA), battery voltage (V), and power (mW).

Table 2. LM-3 12V Test Descriptive Statistics [From Ref 25]

LM-3 12V Test (Feb 8)						
	Battery Current (mA)		Watts (mW)		Battery Voltage (V)	
	Standard	PVPC	Standard	PVPC	Standard	PVPC
Mean	18.06	52.67	206.38	614.32	11.43	11.67
Median	10.00	50.00	114.30	586.50	11.43	11.68
Range	50.00	100.00	571.50	1169.00	0.00	0.14
Minimum	0.00	0.00	0.00	0.00	11.43	11.59
Maximum	50.00	100.00	571.50	1169.00	11.43	11.73
Sum	325.00	948.00	3714.75	11057.82	205.74	209.99
Count	18	18	18	18	18	18

First, we will review and compare the data elements for the current in the battery. The averages can be compared by looking at the mean of each solar power system. For both the Typical and PVPC panels, the average battery currents are 18.06 mA and 52.67 mA, respectively. The two means differ by 34.6 mA which shows an estimated 191% difference by dividing it by 18.06%. Each system has a minimum value of 0.00 mA and a maximum value of 100.0 mA for the PVPC panel, showing a 100% improvement over the typical panel. Summing all the data for a total of 18 readings gives us a total of 325 mA for the typical panel and 948 mA for the PVPC panel. Again, the difference between the two values divided by the sum of all the typical panel currents gave us 191%.

The data elements were reviewed and compared the same way as above for power measured in mW. Again, both the typical and PVPC panel shows minimum value of 0.00 mW and a maximum value of 1169 mW for the PVPC panel. The Typical panel ranges from 0.000 mW to 571.50 mW while the PVPC panel ranges from 0.00 mW to 1169.00 mW. For both the Typical and PVPC panels, the average battery power is 206.38 mW and 614.32 mW, respectively. The two means differ by 407.9 mW which shows an estimated 197% difference by dividing it by 206.38mW. Summing all the data for a total of 18 readings gives us a total of 3714.75 mA for the typical panel and 11057.8 mA for the PVPC panel. The difference between the two values divided by the sum of all the typical panel currents resulted in 197% correlating to the increase in average power.

The table above also shows an initial charge of 11.43 V for the typical panel and 11.67 V for the PVPC panel, resulting with a fully discharged threshold for the battery configuration. Throughout the test, the typical panel's battery charge stayed the same at 11.43 V while the PVPC increased to 11.73 V. This also shows a range of 0 V to 0.14 V for the typical panel and the PVPC panel, respectively. This means that the PVPC panel increased the charge of the battery while the standard system failed to increase the charge.

From the below table and starting from the left, the data collected begins from 0730 with 0.00 mW generated, and then by 0845, the system with PVPC is producing nearly twice the power produced with just the standard system. At 0915, both systems

reached their maximum power output, and continue to produce more than twice as much power as the typical system. A sudden drop in power was seen at 1245 hrs due to a brief period of cloud which in turn caused the sudden reduction in power. The comparison shows that under the severely degraded light conditions the power output for the standard system dropped by 80% from 571 mW to 114 mW. While with the PVPC panel's drop in power was only 50% from 1166 mW to 583 mW. In addition, in these low light conditions, the PVPC panel generated more power (583 mW) than the maximum power output recorded for the typical panel (571 mW) during the entire test period. Lastly, the graph also shows that the PVPC panel continued to produce power for more than an hour and a half after the typical panel stopped producing power.

Table 3. LM3 12V Test PVPC Charging Interval. Test Data at sunrise to sunset showing the difference with the technology incorporated [From Ref 25]

LM3 12V Test (Feb 8)						
Time	Standard System			PVPC System		
	mA	V	mWatts	mA	V	mWatts
0730	0	11.43	0	0	11.59	0
0800	0	11.43	0	4	11.59	46.36
0830	10	11.43	114.3	4	11.59	46.36
0845	25	11.43	285.75	40	11.59	463.6
0915	50	11.43	571.5	100	11.59	1159
0920	50	11.43	571.5	100	11.60	1160
1000	50	11.43	571.5	100	11.59	1159
1200	50	11.43	571.5	100	11.66	1166
1245	10	11.43	114.3	50	11.66	583
1315	50	11.43	571.5	100	11.69	1169
1345	20	11.43	228.6	75	11.73	879.75
1430	10	11.43	114.3	75	11.73	879.75
1515	0	11.43	0	50	11.73	586.5
1545	0	11.43	0	50	11.73	586.5
1615	0	11.43	0	50	11.73	586.5
1645	0	11.43	0	50	11.73	586.5
1715	0	11.43	0	0	11.73	0
1716	0	11.43	0	0	11.73	0

The graphs below depict the collected data for visual comparison of both systems. Figures 31 and 32 show all the data collected for current against time and the power versus time, respectively. The third graph (Figure 33) shows both the current and power plotted against time with the current axis displayed on the left and the power axis displayed on the right.

The significance about the figure is that during the mid-afternoon when there was some brief cloud coverage during the experiment, there was a corresponding drop in power output, as expected. Yet even with that power loss, the percentage of power output was still higher, about 30%, with the technology incorporated, compared to without the technology.

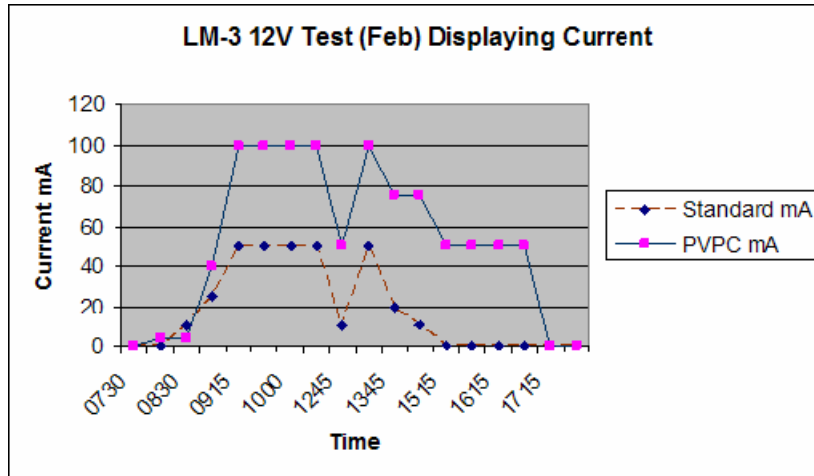


Figure 31. LM-3 12V Test mA Comparison Graph showing the difference with the technology incorporated [From Ref 25]

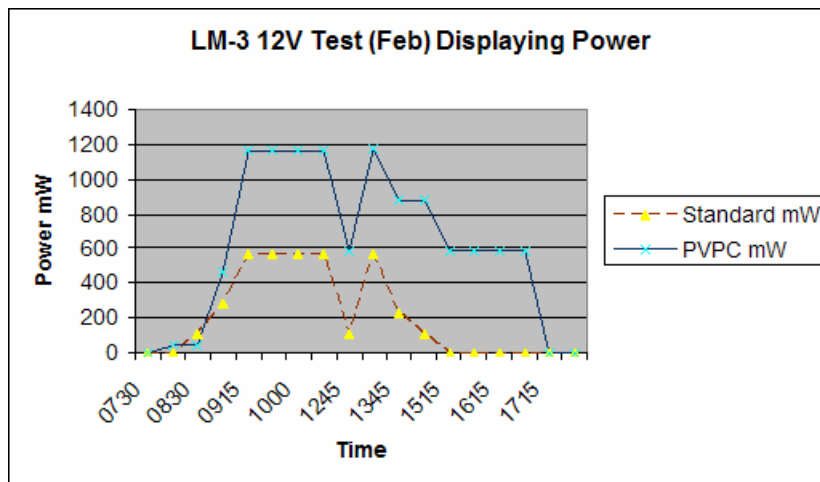


Figure 32. LM-3 12V Test mW Comparison Graph [From Ref 25]

Figure 33 depicts all four data elements. With all four data elements displayed, the current and power for each system follow identical relative paths. The relative numerical differences between the voltage readings for each battery are very small and the same recorded times for the data samples. As a result, current and power are directly

correlated and the relative intervals with relation to the x-axis are identical. It graphically depicts the data collected for power as measured in mW against time.

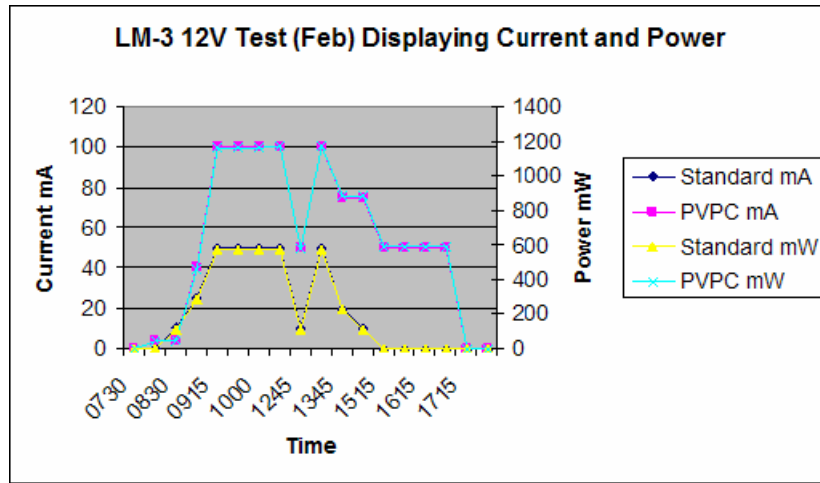


Figure 33. LM-3 12V Test mA and mW Combined Comparison Graph [From Ref 25]

2. LM-3 Test with Programmable Fixed Load

The Uni-Solar LM-3 modules and the HP 6063B DC Programmable Electronic Load system were used to conduct this test. This is done to eliminate any concerns or notion of any slight variation in initial battery voltage biasing the results. Aтира conducted the Programmable Fixed Load (PFL) tests.

To apply a consistent and specified load source, the programmable DC load bank HP 6063B was used simultaneously. The typical and PVPC panels need to be under identical conditions at the beginning of the test to measure the power output. The test started with a load of 0.5 V, and incrementally increasing the loads by 0.5 V until they reached a maximum load of 16.5 V for each system. A 0916 PVPC circuit board was used for the test. Table 4 below displays the data for the test.

To analyze this test result, we consolidated the actual differences between each system and the comparable percentages into the detailed table. We use the same procedure in the section above to calculate these differences and percentage described.

Table 4. LM-3 w/ Programmable Fixed Load Test Descriptive Statistics [From Ref 25]

LM-3 Flex Test w/ Programmable Fixed Load								
	Battery Current (mA)				Watts (mW)			
	Standard	PVPC	Diff	% Diff	Standard	PVPC	Diff	% Diff
Mean	127.27	213.94	86.67	68.10%	707.73	1102.88	395.15	55.83%
Range	210.00	790.00	580.00	276.19%	1620.00	1305.00	-315.00	-19.44%
Minimum	0.00	0.00	0.00	0.00%	0.00	0.00	0.00	0.00%
Maximum	210.00	790.00	580.00	276.19%	1620.00	1305.00	-315.00	-19.44%
Sum	4200.00	7060.00	2860.00	68.10%	23355.00	36395.00	13040.00	55.83%
Count	33.00	33.00			33.00	33.00		

The maximum output of 1305 mW for the PVPC panel is less than the output of 1620 mW for the typical panel. contrary to the previous test. The data shows that during the loads of 7 V to 10.5, the typical panel generated more power than the PVPC panel as depicted in Table 5. This possibly accounted for the use of the 0916 PVPC circuit, which was never specifically designed to optimize at the LM-3's 9 V input level, but at other times the PVPC panel still produced more power.

Table 5. LM-3 Flex Test w/ Programmable Fixed Load Excerpt [From Ref 25]

LM-3 Flex Test w/ Programmable Fixed Load					
System without PVPC			System with PVPC		
Voltage (V)	Current (mA)	Watts (mW)	Voltage (V)	Current (mA)	Watts (mW)
7	190	1330	7	170	1190
7.5	190	1425	7.5	160	1200
8	190	1520	8	150	1200
8.5	180	1530	8.5	150	1275
9	180	1620	9	140	1260
9.5	170	1615	9.5	130	1235
10	160	1600	10	120	1200
10.5	140	1470	10.5	120	1260

Once more, we use the graph to visually compare the data collected for both systems. Figure 34 shows current and power versus the volts or load placed on the system for the battery. The current in mA and power in mW are oriented at the right and left y-axis, respectively, while the x-axis shows the load in V. This graphically depicts that although the typical panel produced more power at voltage loads between 7V and 10.5V, overall the PVPC produced 55% more power [25].

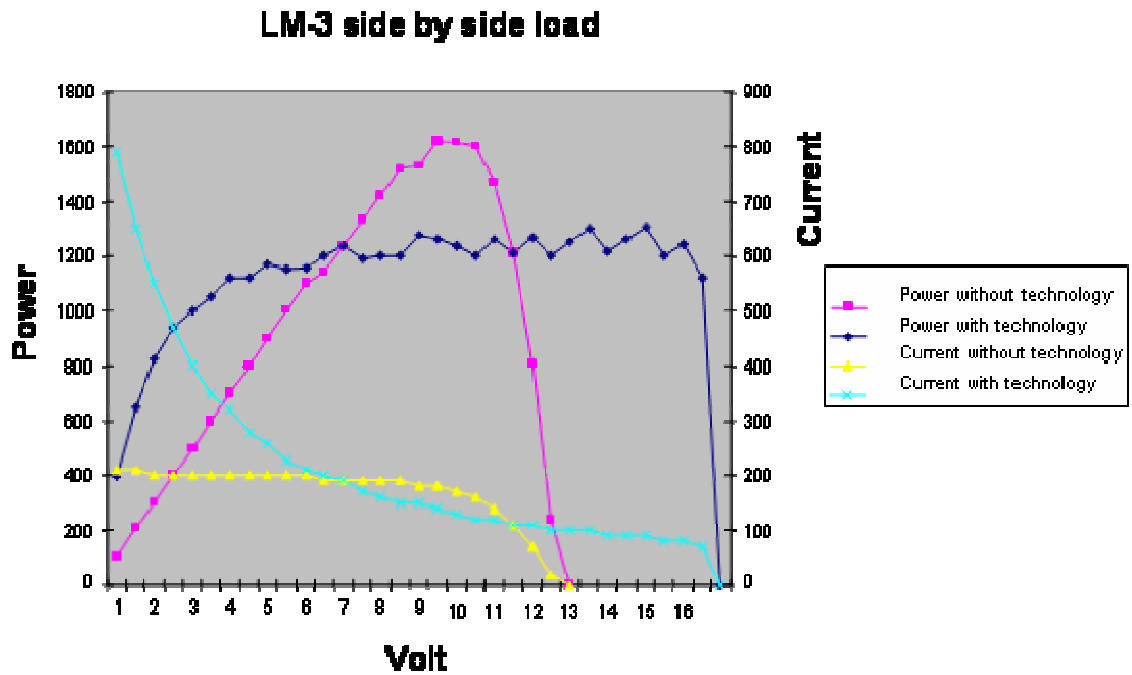


Figure 34. LM-3 Variable Fixed Load Test Graphics [From Ref 25]

C. SUMMARY OF THE TESTS

To conclude whether the solar power system integrated with the PVPC technology generates more power than the typical solar power system, a review and analysis of the results for two separate individual tests is necessary.

The first test conducted during our analyses was the 12V LM-3 Solar Test. The PVPC panel generated an average of 197% more power than the typical panel. The second test was the Atira LM-3 Test with Programmable Fixed Load Battery, which had an overall outcome of 55% more power than the typical panel.

We can simply state that based on the test results depicted in the tables and graphs above for both tests, the PVPC generates more power than the Standard system and the ability to produce power during low light conditions is huge improvement in itself to the typical system.

V. MILITARY APPLICATIONS

A. INTRODUCTION

The successful completion of every mission depends on its ability to communicate, move its personnel expeditiously, and ability to have unlimited power supply for their modern equipment. Such equipment requires significant amounts of power, supplied by heavy disposable and rechargeable batteries. Other alternative power systems are inefficient, unreliable, and most of the time inconvenient to personnel.

In this chapter we will look into a variety of terrestrial applications that can benefit from the PVPC technology to power up rechargeable batteries, including UAV's and perpetual airplane, and the like.

B. SOLDIER POWER REQUIREMENT

The power source that can sustain the electronic equipment necessary in the field for military missions is an important aspect of its accomplishment or extension. Disposable and rechargeable batteries as the primary power source will be discussed in this section to determine existing power requirements. The type of equipment an individual soldier uses and the battery power sources associated with that equipment will be considered to determine how the PVPC can best be utilized to meet individual soldier power needs.

A program called "Objective Force Warrior" by the United States Army is actively seeking technology to facilitate its goal of transforming its troops into a more agile force, seeking to develop and demonstrate revolutionary capabilities that enable the Army soldier to do more while carrying less [19]. A self-sufficient soldier through technology is the main goal of this program but the limitation in power source hinders a more agile force. The program also covers advancements on multifunctional sensors, networked communications, and positioning navigation, among other initiatives.

Tables (6), (7), (8), and (9) came from the Objective Force Warrior Program of the United States Army and listed all the data based on a 5 day mission of a platoon-sized force in field conditions [19]. It details the batteries required for each piece of equipment, and the number of batteries needed each day for each piece of equipment.

The data also listed the power requirement in watt/hours, weight, volume, and cost of batteries associated with each soldier. It requires a total of 933 batteries (Table 6) consisting of seven different types of battery with a total weight of 162 pounds and 3,102 cubic inches in volume (Table 8) at a cost of \$12,991.00 (Table 9) and finally a total power requirement of 11,285 watt/hours (Table 7) for a five day mission of a typical platoon size force. These totals are illustrated below.

Table 6. Platoon Electronic Equipment and Battery Usage 5 day mission analysis. Source from Natick “Objective Force Warrior Program”

5 day mission									
Battery Count	LTWS/PAQ								
	MFI IOS	PFQ/PVS	COO	HTWS/M	PRC126	PRC119	PI GR		
Duty Position	BB516	BA3058 (AA)	BA5123	BA5347	BA5588	BA5590	BA5800	Total	
PL Ldr	1	8	2	10			7	28	
PL Sgt	1	8	2	10	2	4	7	34	
RTO		8	2		2	4		16	
Squad 1	Sqld 1 Ldr		8	2	10	2	7	29	
	Rifle Team A Ldr		8	2				10	
	Grenadier		4	2				6	
	Auto Rifleman		8		10			18	
	Rifleman		88	2				90	
	Rifle Team B Ldr		8	2				10	
	Grenadier		4	2				6	
	Auto Rifleman		8		10			18	
	Rifleman		88	2				90	
Squad 2	Sqld 2 Ldr		8	2	10	2	7	29	
	Rifle Team A Ldr		8	2				10	
	Grenadier		4	2				6	
	Auto Rifleman		8		10			18	
	Rifleman		88	2				90	
	Rifle Team B Ldr		8	2				10	
	Grenadier		4	2				6	
	Auto Rifleman		8		10			18	
	Rifleman		88	2				90	
Squad 3	Sqld 3 Ldr		8	2	10	2	7	29	
	Rifle Team A Ldr		8	2				10	
	Grenadier		4	2				6	
	Auto Rifleman		8		10			18	
	Rifleman		88	2				90	
	Rifle Team B Ldr		8	2				10	
	Grenadier		4	2				6	
	Auto Rifleman		8		10			18	
	Rifleman		88	2				90	
MGO			4					4	
MTWS Extra				20				20	
Total	2	696	52	130	10	8	35	933	

Table 7. Platoon 5 day Battery analysis in Watt/Hours. Source from Natick “Objective Force Warrior Program”

		Energy (Watt-hours)								
		Wh/unit	6	4	4.5	40	35	185	35	(Wh)
No.	Duty Position	BB516	BA3058 (AA)	BA5123	BA5347	BA5588	BA5590	BA5800	Total	
1	PL Ldr	6	32	9	400			245	692	
2	PL Sgt	6	32	9	400	70	740	245	1502	
3	RTO		32	9		70	740		851	
4	Sqd 1 Ldr		32	9	400	70		245	756	
5	Rifle Team A Ldr		32	9					41	
6	Grenadier		16	9					25	
7	Auto Rifleman		32		400				432	
8	Rifleman		352	9					361	
9	Rifle Team B Ldr		32	9					41	
10	Grenadier		16	9					25	
11	Auto Rifleman		32		400				432	
12	Rifleman		352	9					361	
13	Sqd 2 Ldr		32	9	400	70		245	756	
14	Rifle Team A Ldr		32	9					41	
15	Grenadier		16	9					25	
16	Auto Rifleman		32		400				432	
17	Rifleman		352	9					361	
18	Rifle Team B Ldr		32	9					41	
19	Grenadier		16	9					25	
20	Auto Rifleman		32		400				432	
21	Rifleman		352	9					361	
22	Sqd 3 Ldr		32	9	400	70		245	756	
23	Rifle Team A Ldr		32	9					41	
24	Grenadier		16	9					25	
25	Auto Rifleman		32		400				432	
26	Rifleman		352	9					361	
27	Rifle Team B Ldr		32	9					41	
28	Grenadier		16	9					25	
29	Auto Rifleman		32		400				432	
30	Rifleman		352	9					361	
	MGO			18					18	
	MTWS Extra				800				800	
	Total	12	2784	234	5200	350	1480	1225	11285	

Table 8. Platoon 5 day Battery analysis in weight. Source from Natick “Objective Force Warrior Program”

		Weight (lbs.)								
		Weight/battery	0.59	0.051	0.037	0.64	0.63	2.25	0.45	(lbs)
No.	Duty Position	BB516	BA3058 (AA)	BA5123	BA5347	BA5588	BA5590	BA5800	Total	
1	PL Ldr	0.59	0.408	0.074	6.4			3.15	10.622	
2	PL Sgt	0.59	0.408	0.074	6.4	1.26	9	3.15	20.882	
3	RTO		0.408	0.074		1.26	9		10.742	
4	Sqd 1 Ldr		0.408	0.074	6.4	1.26		3.15	11.292	
5	Rifle Team A Ldr		0.408	0.074					0.482	
6	Grenadier		0.204	0.074					0.278	
7	Auto Rifleman		0.408		6.4				6.808	
8	Rifleman		4.488	0.074					4.562	
9	Rifle Team B Ldr		0.408	0.074					0.482	
10	Grenadier		0.204	0.074					0.278	
11	Auto Rifleman		0.408		6.4				6.808	
12	Rifleman		4.488	0.074					4.562	
13	Sqd 2 Ldr		0.408	0.074	6.4	1.26		3.15	11.292	
14	Rifle Team A Ldr		0.408	0.074					0.482	
15	Grenadier		0.204	0.074					0.278	
16	Auto Rifleman		0.408		6.4				6.808	
17	Rifleman		4.488	0.074					4.562	
18	Rifle Team B Ldr		0.408	0.074					0.482	
19	Grenadier		0.204	0.074					0.278	
20	Auto Rifleman		0.408		6.4				6.808	
21	Rifleman		4.488	0.074					4.562	
22	Sqd 3 Ldr		0.408	0.074	6.4	1.26		3.15	11.292	
23	Rifle Team A Ldr		0.408	0.074					0.482	
24	Grenadier		0.204	0.074					0.278	
25	Auto Rifleman		0.408		6.4				6.808	
26	Rifleman		4.488	0.074					4.562	
27	Rifle Team B Ldr		0.408	0.074					0.482	
28	Grenadier		0.204	0.074					0.278	
29	Auto Rifleman		0.408		6.4				6.808	
30	Rifleman		4.488	0.074					4.562	
	MGO			0.148					0.148	
	MTWS Extra				12.8				12.8	
	Total	1.18	35.496	1.924	83.2	6.3	18	15.75	161.85	

Table 9. Platoon 5-day battery analysis in dollars. Source from Natick “Objective Force Warrior Program”

		Dollars (\$)								
		S/battery	110	0.2	2.08	81.83	37.2	79.25	25.13	(\$)
No.	Duty Position	BB516	BA3058 (AA)	BA5123	BA5347	BA5588	BA5590	BA5800	Total	
1	PL Ldr	110	1.6	4.16	818.3			175.91	1109.97	
2	PL Sgt	110	1.6	4.16	818.3	74.4	317	175.91	1501.37	
3	RTO		1.6	4.16		74.4	317		397.16	
4	Sqd 1 Ldr		1.6	4.16	818.3	74.4		175.91	1074.37	
5	Rifle Team A Ldr		1.6	4.16					5.76	
6	Greradier		0.8	4.16					4.96	
7	Auto Rifleman		1.6		818.3				819.90	
8	Rifleman		17.6	4.16					21.76	
9	Rifle Team B Ldr		1.6	4.16					5.76	
10	Greradier		0.8	4.16					4.96	
11	Auto Rifleman		1.6		818.3				819.90	
12	Rifleman		17.6	4.16					21.76	
13	Sqd 2 Ldr		1.6	4.16	818.3	74.4		175.91	1074.37	
14	Rifle Team A Ldr		1.6	4.16					5.76	
15	Greradier		0.8	4.16					4.96	
16	Auto Rifleman		1.6		818.3				819.9	
17	Rifleman		17.6	4.16					21.76	
18	Rifle Team B Ldr		1.6	4.16					5.76	
19	Greradier		0.8	4.16					4.96	
20	Auto Rifleman		1.6		818.3				819.90	
21	Rifleman		17.6	4.16					21.76	
22	Sqd 3 Ldr		1.6	4.16	818.3	74.4		175.91	1074.37	
23	Rifle Team A Ldr		1.6	4.16					5.76	
24	Greradier		0.8	4.16					4.96	
25	Auto Rifleman		1.6		818.3				819.90	
26	Rifleman		17.6	4.16					21.76	
27	Rifle Team B Ldr		1.6	4.16					5.76	
28	Greradier		0.8	4.16					4.96	
29	Auto Rifleman		1.6		818.3				819.90	
30	Rifleman		17.6	4.16					21.76	
	MGO			8.3						
	MTWS Extra				1636.6				1636.00	
	Total	220	139.2	108.16	10637.9	372	634	879.55	12990.81	

This is where the PVPC technology comes in to provide a reliable and efficient power source compared to the current practice of using disposable batteries and generators. This PVPC technology can sustain the needed power levels continuously over extended periods of time in operational environments. This technology not only solves the power requirements of the Objective Force Warrior program, it can save millions of dollars as compared to the current practices using generators and batteries [19].

a. Typical Equipment

The following are the typical equipment being used by the military in the field:

- NVG's
- IR Aiming Lights
- GPS/ BA-3058
- Tactical Light/ DL-123A
- Thermal Sights/BA5590

b. Equipment That Uses the BA-5590 or Equivalent



Figure 35. AN/PRC-119F (SINCGARS) [From Ref 19]



Figure 36. AN/PSC-5 Tactical Satellite Telephone/Radio [From Ref 19]



Figure 37. AN/PRC-117F Secure Tactical Radio [From Ref 19]



Figure 38. AN/PRC-150 VHF Radio [From Ref 19]



Figure 39. Chemical Sensor [From Ref 19]

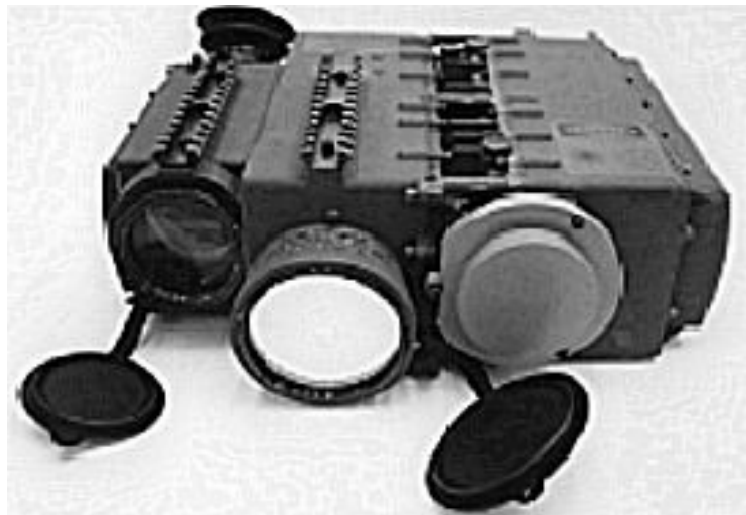


Figure 40. Laser Target Identifier [From Ref 19]



Figure 41. Laser/Rangefinder [From Ref 19]



Figure 42. M98A1 Javelin Missile System [From Ref 20]

c. Battery Chargers

Alternative to the use of BA-5590 batteries are rechargeable batteries. Initial power source is required to charge these batteries and below are two kinds of chargers available in the market.



Figure 43. PP-8494 Battery Charger [From Ref 19]



Figure 44. PP-8444 Battery Charger [From Ref 19]



Figure 45. PVPCT System Prototype With Flexible Solar Array Deployed [From Ref 20]

C. PERPETUAL AIRPLANE

A solar-powered drone called SoLong successfully flown for 48 hours non-stop was developed by Alan G. Cocconi of a small research company, AC Propulsion located in San Dimas, California. Powered by solar cells built into its wings, it weighs 28.2 lbs, has a 15.6 ft wing span, takes off with its own 1-hp motor from a wheeled dolly and is capable of climbing up to 50,000 feet [21]. Lithium-ion laptop computer batteries can be used to store energy during the day which allows the aircraft to continuously fly at night. In addition, small near-term improvements in the design and better batteries in the future could possibly permit the aircraft to stay in flight for months. Other application of this technology is for UAV or acting as a radio tower in the sky, giving line-of-sight access across a city or area [21]. It is well equipped with a control system of sophisticated autopilot with inertial, barometric and GPS references, a television camera giving a pilot's eye view. Although the aircraft is small, its flight system is comparable to those larger aircraft.



Figure 46. Alan Cocconi with SoLong at El Mirage Dry Lake in California. [From www.acpropulsion.com/ACP_PDFs/ACP_SoLong_Solar_UAV_2005-06-05.pdf]. Last accessed September 2005.

1. Limitations

This major achievement does not come easy and there are limitations that need to be considered for further development. Cocconi pointed out that there was no mission

flexibility. During the day, the battery requires most of the solar power put into it, thus it soared and glided to keep the motor off most of the day. The battery also has less energy per pound.

There was no payload except for the TV camera for a simple reconnaissance. It requires a cloud-free sky and reasonable weather to sustain its continuous flight. This is where the PVPC will be most beneficial to this aircraft, since the technology can provide power during the day even in low light conditions.

2. Improvements

The aircraft is fairly tough and has flown in 30 mph winds and some desert turbulence. In sixty plus flights and over 250 hours of flying, it has never been seriously damaged. Its battery stored plenty of energy to continuously stay aloft for a third night and possibly a fourth or a fifth except the pilot was too tired to continue the test. After the two nights of flight, the battery charge was only down less than 5%.

Cocconi's plan is to concentrate on a multi-day flight, then build from this to improve the aircraft. Some of the key parameters needed are the energy density of the batteries, efficiency of the solar cells, and other things like round-trip battery storage and motor economy during loiter thrust.

Major technology improvements are coming in solar cells, batteries, and the power converter. SoLong was initially fitted with 100 LG Chem 18650-size lithium-ion laptop cells storing 185 watt-hr per kilogram, totaling 800 watt-hr, but the battery was not quite big enough for a full night and could not absorb all the day's solar energy. So, after receiving the Sanyo 18650 cells that could hold 214 watt-hr./kg., a 15% improvement, and also increasing the number of batteries to 120 cells, the aircraft is now on its tipped performance, barely capable of multi-day flights.

SoLong is currently using Sunpower A300 single-crystal silicon solar cells which have about 20% efficiency. Covering about 13 square feet, each wing contains a series of 38 cells generating a nominal 225 watts, weighing about 2.3 lb. More expensive space-grade solar cells are now available like the triple-junction cells with 26.5% efficiency [33] that can provide approximately 40% more power. The triple junction (TJ) cells are about 100 times more expensive so covering the wing span would cost around \$150,000.

The next generation of batteries and boost in power would make SoLong a multi-day airplane with no glider soaring required. Solar cell prices can only go down, and the reality of this craft is close. Cocconi is planning on building a larger aircraft that can fly higher, but both those objectives would make the job more difficult and require bigger improvements in solar cell efficiency, battery energy density and lightweight structure [21].

D. UNMANNED AERIAL VEHICLES (UAV)

Currently twenty-two companies within the U.S. are or have been involved in the development and production of UAV's. Also, there are approximately forty-five different UAV configurations. The tables and figures below list the categories and capabilities for most of them. The Global Hawk shown in Figure 46 is one of the most advanced and high-endurance type of UAV.



Figure 47. Global Hawk [from Ref 22].

Table 10. UAV Capabilities [From Ref 22]

UAV Name	Endurance	Payload Weight	Altitude
Aerosonde	40 hrs.	2.2 lbs.	20,000 ft.
Altus2	24 hrs.	330 lbs.	65,000 ft.
BQM-34	1.25 hrs.	470 lbs.	60,000 ft.
Exdrone	2.5 hr.	25 lbs	10,000 ft.
Global Hawk	42 hrs.	1,960 lbs.	65,000 ft.
Gnat 750	48 hrs.	140 lbs.	25,000 ft.
Pioneer	5.5 hrs.	75 lbs.	12,000 ft.
Shadow 200	4 hrs.	50 lbs.	15,000 ft.

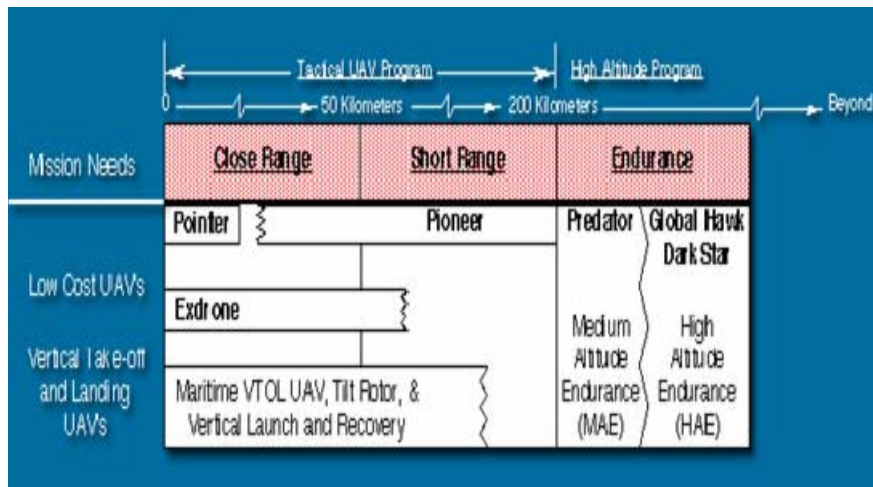


Figure 48. Categories of UAV [From Ref 22]

Table 11. Categories of UAV [From ref 22]

Other U.S. UAV Development/Production Activity		
Local	Regional	Endurance
Shadow 200	Shadow 600	Chiron
AV Pointer Micro Bimp	Truck	BQM-34
SASS Lite Blimp	Skyeye	Model 324
Javelin	Eagle-Eye	Model 350
Porter	Aerobat (A24-2)	Model 410
Tem	Spectre II	GNAT 750
H-7B	Seabat	Altus I
H-7F	S-Tec Sentry	Altus II
H-7H	Hunter	Pathfinder
Freewing Tilt-Body	Outrider	Perseus B
Huntait		Raptor
Prowler		Thesues
Flash		Helios
HIT		
Aerobot (FS-24)		
Aerosonde		
Cyper		
X AP		

The SoLong aircraft with small adjustments in its design and size can easily be applied to Unmanned Aerial Vehicles (UAV).

E. OTHER USES

Some of the possible uses for the PVPC technology are listed below.

1. Power utility grid that can provide electricity for a large area acting as a primary or back-up power source. Detailed reading on information on how this is possible can be taken from a MBA professional report on (Naval Postgraduate School, June 2005) “A Study Examining Photovoltaic (PV) Solar Power as an Alternative for the Rebuilding of the Iraqi Electrical Power Generation Infrastructure” by C. Austin, R Borja, and J Phillips [26].
2. Most stock class solar cars use commercially available terrestrial grade silicon cells. It consists of numerous individual cells (approaching 1000) to form the "solar array". These arrays generally work between 50 and 200 volts, and can provide up to around 1000 watts of power, depending on the electric motor used to drive the car. A lot of factors affect the array’s output such as the intensity of the sun, cloud cover, and temperature. Space grade solar cells are used by many teams for open class solar cars. These cells are generally smaller and much more expensive than the conventional silicon cells. They also are more efficient [12].

F. SUMMARY

For field military personnel on a mission in remote areas, the ability to have uninterrupted communications and use of their equipment from unlimited available power sources are critical for their survival. The PVPC technology can make a more self-sufficient and mobile soldier. They will be less reliant on supply chains by carrying lesser combat load due to elimination of unnecessary non-rechargeable batteries to power their equipment.

Intelligence can make or break the outcome of a mission or war. Incorporating the PVPC technology to current development in aviation especially to the very promising SoLong aircraft or other UAV prototype can provide us with unlimited information on any area of interest. Other military applications can benefit substantially from this new technology as proven from all the test results. In short, PVPC 's ability to provide more power can have a significant impact in the way our military conducts its missions.

VI. SPACE APPLICATIONS

A. INTRODUCTION

This chapter will look into the Naval Postgraduate School Spacecraft Architecture and Technology Demonstration Satellite (NPSAT1) as a model for the PVPC's space applicability. NPSAT1 is the follow-on spacecraft to the PANSAT. It is a low-cost technology demonstration satellite sponsored by the Department of Defense (DOD) Space Test Program (STP) and will be one of five satellites to be launched on an Atlas V Evolved Expendable Launch Vehicle (EELV) in late 2006. NPSAT1 currently holds nine experiments, seven of which are being developed by the Space Systems Academic Group.

This chapter will present an approach for improving spacecraft available power using an advanced solar panels maximum power tracking circuit. The design is being proposed for integrating onboard the Naval Postgraduate School's soon-to-be-launched satellite (NPSAT1) or for future satellite launches.

B. SPACECRAFT ARCHITECTURE

The NPS Spacecraft weighs approximately 180-lbs, is a twelve-sided, semi-cylindrical satellite covered with solar panels on each of the 12 surfaces. The solar cell array is divided into three rings: top, middle, and bottom ring. Both ends of the spacecraft have mounted antennas to allow constant communications with the ground station even at times when the satellite is not pointing directly towards earth. NPSAT1 will be injected into a circular orbit of 560 km and 35.4 degrees inclination, providing for an orbital period of 95.8 minutes, or about 16 orbits per day.

The EELV Secondary Payload Adapter (ESPA) is the mechanism used to attach NPSAT1 to the launch vehicle. It will be powered off while attached to the launch vehicle and will be powered on upon separation. Ground station communications will be established shortly after and initial spacecraft telemetry will be then be received.

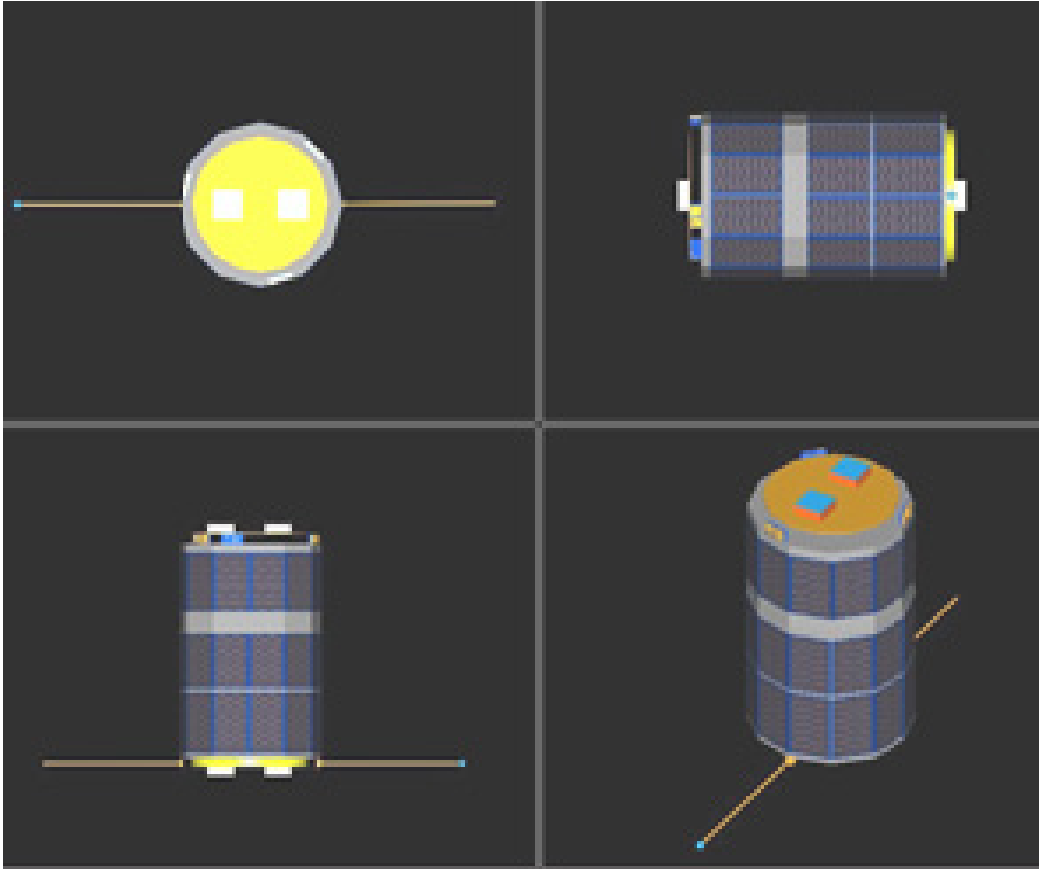


Figure 49. Computer generated model of NPSAT1. Note the three “rings” of solar arrays [From Ref 30]

C. ON BOARD SUBSYSTEMS

NPSAT1 is comprised of four major subsystems: the Command and Data Handler (C&DH), the Electrical Power Subsystem (EPS), the Attitude Control Subsystem (ACS), and the Radio Frequency Subsystem. Each of these major subsystems is described in the figure below.

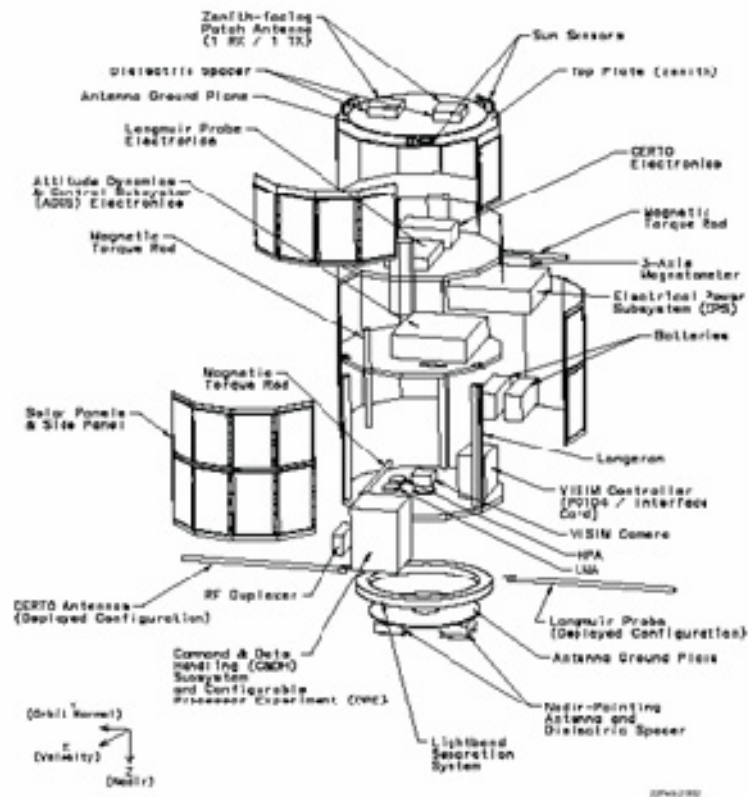


Figure 50. NPSAT1 expanded view of Payload and Subsystems [From Ref 30]

1. Command and Data Handler (C&DH) Subsystem

The C&DH is considered to be the brain of the spacecraft and is used in controlling the other subsystems. It contains a motherboard, an analog-to-digital conversion circuit, the Configurable Fault-Tolerant Processor experiment (CFTP), RFS components, and data storage. A low power Advanced Reduced Instruction Set Computer (RISC) Machine (ARM) processor running on Linux operating system is used with 256 megabytes of memory for data and telemetry storage.

2. Electrical Power Subsystem

The Triple-Junction solar cells, lithium-ion (Li-ion) batteries, and control electronics comprise the EPS. The top and bottom rings of the spacecraft use the SPECTROLAB Improved Triple Junction (ITJ) cells to provide power and charge the batteries.

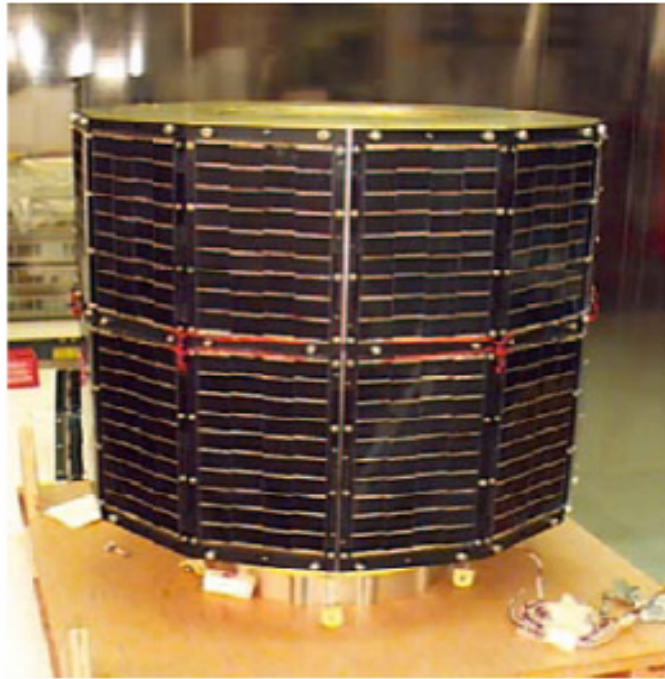


Figure 51. NPSAT1 Solar Cell Array – Early Stage with Silicon Cells [From Ref 32]

3. Attitude Control Subsystem

The spacecraft's three-axis stabilization controllability will be provided by the Attitude Control Subsystem (ACS). Magnetic torque rods are used as actuators and a three-axis magnetometer is used as a sensor. For backup stability, a momentum wheel is used. In order to obtain the satellite's location, the ACS uses orbit information, performs a table look-up for the magnetic field vector at that particular location, and compares it to the magnetometer measurement. The torque rods are used to correct any differences.

4. Radio Frequency Subsystem

A 100-kbps full duplex system is used for both uplink and downlink transmissions. The modem is a commercial off-the-shelf (COTS) device and will operate at 1767.565 MHz for uplink and at 2207.3 MHz for downlink using 70-MHz IF.

D. PAYLOAD/MISSION EXPERIMENTS

Several experiments will be conducted aboard the NPSAT1, several of which are NPS theses, which can prove to be very beneficial to the school's space systems research.

1. CERTO and Langmuir Probes

Coherent Electromagnetic Radio Tomography (CERTO) and Langmuir probes on rockets and satellites are used to measure electron and ion densities and electron

temperatures in the ionosphere. The data gathered from this experiment can be used to develop tomographic algorithms for reconstruction of ionospheric irregularities.

2. Configurable Fault-Tolerant Processor (CFTP)

The CFTP is a Triple-Modular Redundant (TMR) configurable processor that can mitigate single event upsets (SEU) when the processor is vulnerable to unintentional bit flips while exposed to harsh radiation in space. A Field Programmable Gate Array (FPGA) will be programmed to act as a TMR processor and has the capability to be reconfigured.

3. Visible Wavelength Imager (VISIM)

VISIM is a COTS digital camera with a resolution of 652 x 494 pixels and will have a field view of about 200 x 150 km when the spacecraft is on orbit at 560 km. Images taken will be in JPEG format and the ground controller can decide to download the raw images on the next pass of the satellite.

4. Solar-Cell Measurement System (SMS)

This is an NPS experiment with a goal of gathering data from new, experimental solar cells in space. The system will gather time-stamped I-V curves along with temperature and sunlight angle information.

As mentioned earlier, the XTJ cells are mounted on the 12 panels of the middle ring to provide power to the spacecraft. Two additional cells are mounted near the top of the twelve panels for the sole purpose of the SMS experiment. Of the 24 additional cells, 2 will be space qualified dual junction cells used for reference. Only 22 experimental cells are used for data gathering

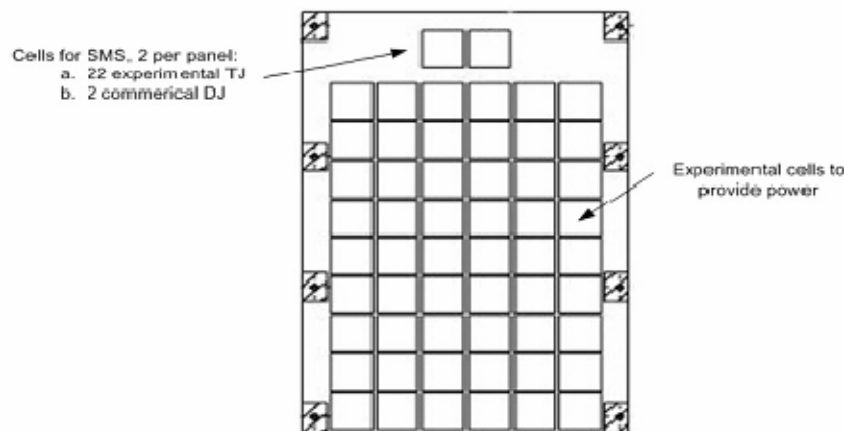


Figure 52. Middle Ring Solar Cell Array Layout [From Ref 1]

E. POWER SOURCES

1. Lithium-Ion Batteries

Lithium-Ion rechargeable batteries are advantageous for space use because they offer the highest energy density (Watt-hours per kilogram) than any of the battery technologies currently used in space. These batteries already have over-charging and excessive load protection circuitry built in. As a result, no extra space is needed for the placement of extra batteries and this minimizes unnecessary cost and maintenance.

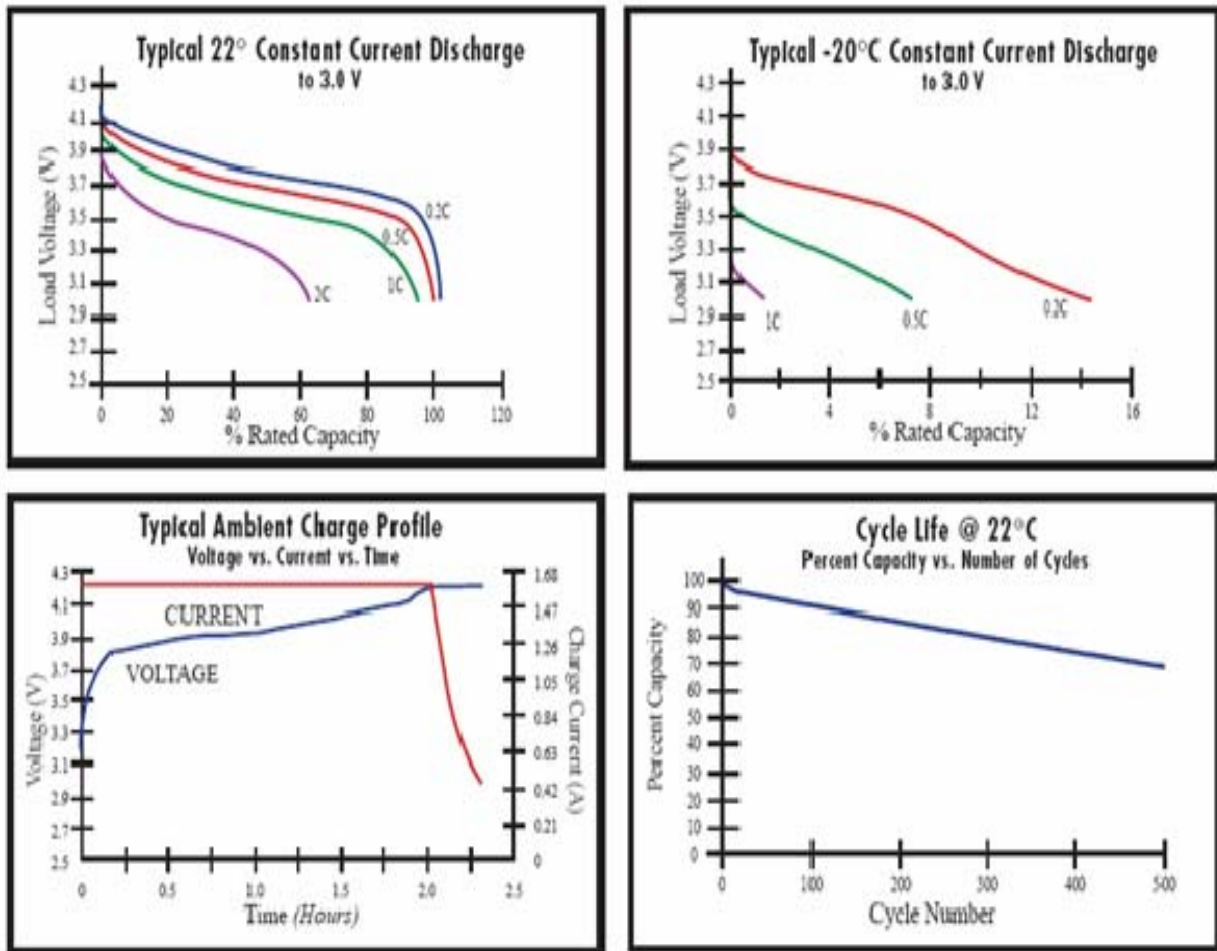


Figure 53. Lithium-Ion Batteries Charge/Discharge Chart [From Ref 33]

Table 12. Lithium-Ion Battery Data Table [From Ref 33]

Voltage Range:	3 to 4.2 V										
Average Voltage:	3.7 V										
Nominal Capacity:	3.3 Ah @ C/5 Rate @ 23° C										
Max. Discharge:	2.5 A continuous										
Pulse Capacity:	Varies according to pulse characteristics, temperature, cell history and the application. Consult Ultralife.										
Energy:	12.1 Wh										
Energy Density:	142 Wh/kg, 277 Wh/l										
Weight:	85 Grams										
Cycle Life:	> 300 cycles @ C/5 to 80% of initial capacity										
Memory:	No Memory Effect										
Operating Temp.:	-20° C to 60° C										
Storage Temp.:	-20° C to 60° C										
Self-Discharge:	< 10% per Month										
Exterior/Housing:	Laminated Foil										
Terminals/Connector:	22 AWG Wire: Red (+), Black (-)										
Safety:	Material Safety Datasheet - MSDS014.										
Transportation:	Excepted from Regulations - see note 1.										
Protection Circuit Module:	<table> <tr> <td>Over Voltage Limit:</td> <td>4.275 +/- 0.03 Volts</td> </tr> <tr> <td>Under Voltage Limit:</td> <td>2.3 +/- 0.08 Volts</td> </tr> <tr> <td>Over Current Protection:</td> <td>3.5 A @ Room Temperature</td> </tr> <tr> <td>Max. Quiescent Drain:</td> <td>20 μA</td> </tr> <tr> <td></td> <td><</td> </tr> </table>	Over Voltage Limit:	4.275 +/- 0.03 Volts	Under Voltage Limit:	2.3 +/- 0.08 Volts	Over Current Protection:	3.5 A @ Room Temperature	Max. Quiescent Drain:	20 μ A		<
Over Voltage Limit:	4.275 +/- 0.03 Volts										
Under Voltage Limit:	2.3 +/- 0.08 Volts										
Over Current Protection:	3.5 A @ Room Temperature										
Max. Quiescent Drain:	20 μ A										
	<										
Charging:	Maximum charge rate at C/2 to 4.2 Volts in a temperature range of 0° to 45° C. Hold at 4.2 Volts until current declines to C/10. Refer also to Safety Guide UBI-5112.										

2. Improved Triple Junction Solar Cells

The SPECTROLAB Improved Triple Junction (ITJ) solar cells were selected for use on NPSAT1. The ITJ solar cells are proven to be the most efficient and most optimal solar cells to be used on NPSAT1. The other solar cells considered were Silicon and Gallium Arsenide solar cells. The basic construction of an ITJ cell is comprised of Gallium Indium Phosphide, Gallium Arsenide, and Germanium solar cells.

Table 13. Improved Triple Junction Solar Cells Electrical Parameters [From Ref 34]

Typical Electrical Parameters (AM0 (135.3 mW/cm ²) 28°C, Bare Cell)			
J _{sc} = 16.90 mA/cm ²			
J _{mp} = 16.00 mA/cm ²			
J _{load min avg} = 16.10 mA/cm ²			
V _{oc} = 2.565 V			
V _{mp} = 2.270 V			
V _{load} = 2.230 V			
Cff= 0.84			
Eff _{load} = 26.5%			
Eff _{mp} = 26.8%			
Radiation Degradation (Fluence 1MeV Electrons/cm ²)			
Parameters	1x10 ¹⁴	5x10 ¹⁴	1x10 ¹⁵
I _{mp} /I _{mp0}	1.00	0.98	0.96
V _{mp} /V _{mp0}	0.94	0.90	0.88
P _{mp} /P _{mp0}	0.94	0.88	0.84
Thermal Properties			
Solar Absorptance= 0.92 (Ceria Doped Microsheet)			
Emittance (Normal)= 0.85 (Ceria Doped Microsheet)			
Weight			
84 mg/ cm ² (Bare) @ 140 μm (5.5 mil) Thickness			
Thickness of 175 μm typical with weight equivalence of a 140 μm thick cell.			
Temperature Coefficients (10°C - 80°C)			
Parameters	BOL	1x10 ¹⁵ (1 MeV e/cm ²)	
J _{mp} (μA/cm ² /°C)	7.3	9.5	
J _{sc} (μA/cm ² /°C)	11.5	12.4	
V _{mp} (mV/°C)	-6.2	-6.6	
V _{oc} (mV/°C)	-5.9	-6.5	

Typical IV Characteristic
AM0 (135.3 mW/cm²) 28°C, Bare Cell

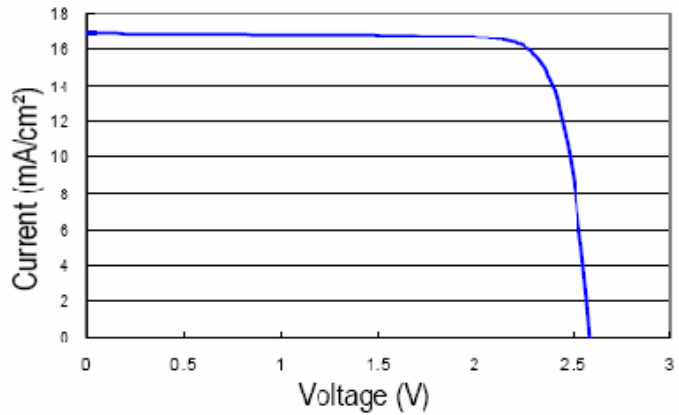


Figure 54. Improved Triple Junction Solar Cell I-V Curve [From Ref 34]

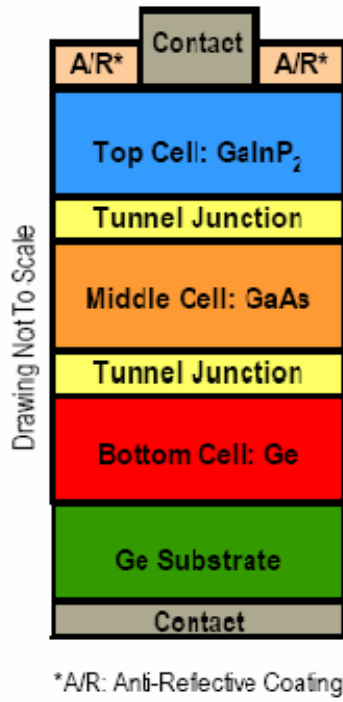


Figure 55. Simplified cross-sectional view of Improved Triple Junction Solar Cell Layers [From Ref 34]

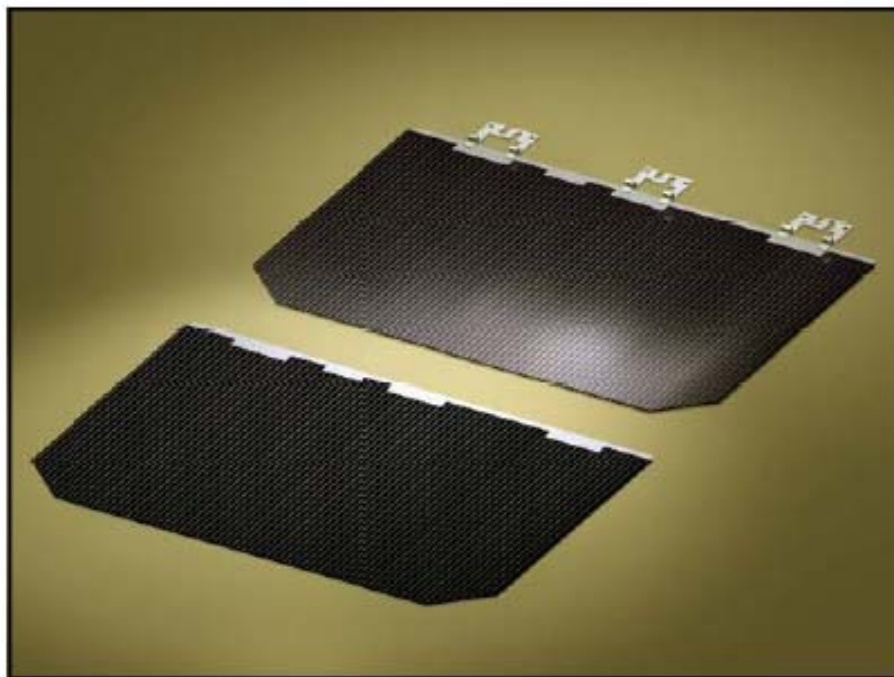


Figure 56. SPECTROLAB Improved Junction Solar Cells [From Ref 34]



Figure 57. Some of the solar cell panels for NPSAT1, populated with Spectrolab ITJ cells (photo courtesy of Spectrolab).

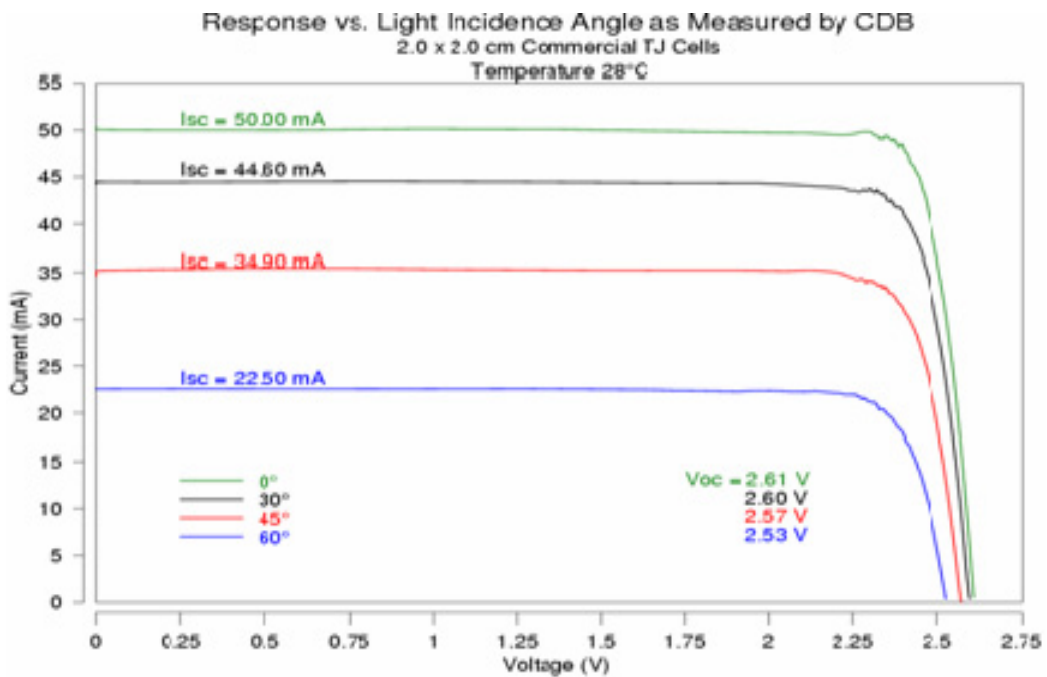


Figure 58. *I-V* curves of an ITJ cell for various incidence angles, taken by CDB, cell at 28°C [From Ref 1]

As stated earlier, the three panels for each side are covered by 15 cells per panel connected in series, giving a total of 45 cells per side of the satellite. The adjacent side panels are at an angle of 30 degrees, 60 degrees, and 90 degrees from the horizontal

provided that the sun is directly perpendicular to one of the side panel at an instance to simplify calculation. To determine the maximum power output for the NPSAT1 using the improved triple junction cells, the cell layout as described in Figures 49 and 50 and the number of cells are used in the calculation below

$$\text{Cell Area} = 3 \text{ cm} \times 4 \text{ cm} = 12 \text{ sqcm}$$

$$\text{Total Effective Area per panel} = 12 \text{ cm} \times 15 \text{ cm} = 180.0 \text{ sqcm}$$

$$\text{Total Effective Area per side} = 180 \text{ sqcm} \times 3 \text{ panel} = 540 \text{ sqcm}$$

$$\text{Maximum Power} = 540 \text{ sqcm} \times .135\text{W/sqcm} = 72.9 \text{ W}$$

$$\text{@ 0 degrees} = 72.9 \text{ W}$$

$$\text{@ 30 degrees} = 72.9 \text{ W} * \cos (30) = 63.13 \text{ W}$$

$$\text{@ 60 degrees} = 72.9 \text{ W} * \cos (60) = 36.45 \text{ W}$$

$$\text{@ 90 degrees} = 0 \text{ W}$$

$$\text{Total Maximum Power} = 172.48 \text{ W}$$

$$\text{Maximum Power/side} = 172.48 * 26.5\% = 45.71 \text{ W}$$

F. AS A RESERVE BACKUP POWER

NPSAT1 requires a relatively high amount of power in order to perform all of the experiments it is intended to do. Unfortunately, it would not be fully exposed to the sun at all times as it orbits around the sun. From the table below, the total average energy per orbit is approximately 18.3 W-hr and the solar panel on board the satellite is able to provide 21.2 W-hr per orbit. From these characteristics it is obvious that some sort of a back-up power source is necessary. Improving on the fundamentals of solar power conversion technology, a prominent power conversion company called Aтира Technologies proposes a new and improved power conversion technology that allows for the capability of charging a battery and use it as a back-up power source, in addition to the main power source, to be used aboard the NPSAT1.

The NPSAT1 spacecraft is expected to receive limited solar panel power output. In order to budget the power requirements of all the experiments on board, duty-cycling of the satellite's sub-systems is required. The average power requirement for the payloads and subsystems is tabulated below.

Table 14. Estimated NPSAT1 Power Budget Requirement [From Ref 28]

Subsystem / Component	Duty Cycle (%)	Avg. Power (W)	Avg. Energy/Orbit (W-hr)
EPS Processor Board	50	.75	1.20
Switch Board A/D	50	.03	.05
Switch Board DAC	50	.03	.05
Switches	100	.50	.80
ACS Torque Rods	50	.02	.02
Processor Board	50	.75	1.2
Magnetometer	10	.14	.22
MEMS	1	.02	.04
C&DH 386 Core	50	.80	1.28
EDAC RAM	25	1.02	1.63
SCC	100	.08	0.13
UART	100	.23	0.37
FPGA	100	.25	0.40
Solid State Disk	50	.15	0.24
A/D	100	2.05	3.27
RFS TX/RX	2	.30	.48
LO (& modem)	3	.09	.14
SMS (only operates in sunlight)			
Processor Board	5	.12	.12
Switch Board A/D	5	.01	.01
Switch Board DAC	5	.005	.005
CERTO Standby	12.5	.43	.69
150/400 MHz mode	20	1.53	2.43
1067 MHz mode	6.6	.34	.54
Langmuir probe	26.5	.42	.68
Configurable Processor Exp.	25	1.00	1.60
VISIM (only operates in sunlight)	8.5	.68	.68
Total Average Energy per Orbit			18.3
Solar Panel Energy (75% eff.)			21.2
Margin (W-hr)			3.0

Unfortunately, solar cells only provide a certain amount of energy, typically computed in the form of efficiency, between the range of 11% and 20%. Furthermore, from the power equation, $P = IV$, where P is power, I is current, and V is voltage, the maximum power generated happens only at a particular point on a typical I-V curve, called the knee. The figure below depicts an I-V curve characteristic of a typical solar cell, showing the Battery Changing Window. In other words, this window indicates the optimum power point, particularly when the panel is in full sunlight.

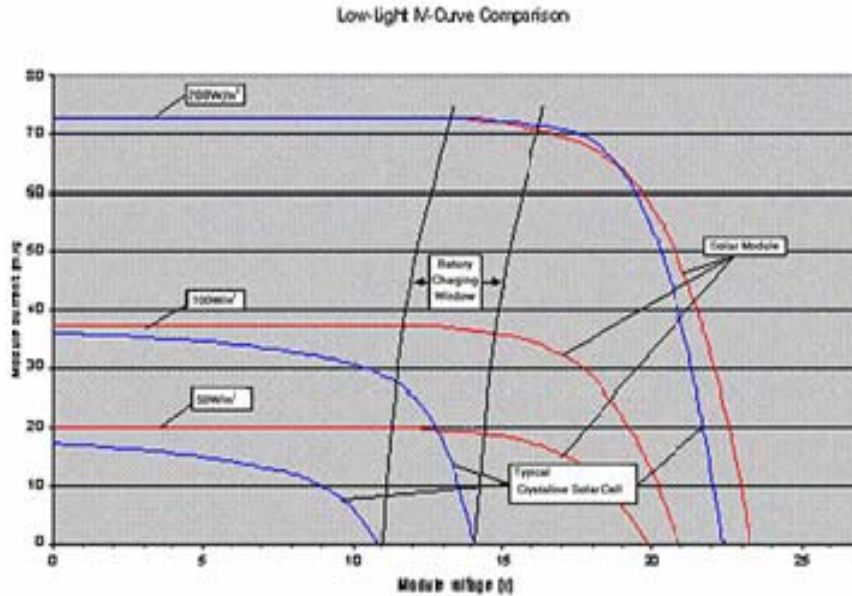


Figure 59. I-V Characteristic Curve showing the Low Light Effect on Battery Charging. (From www.solengy.com/pages/whitepapers.html, July 2005)

Looking closely at the above figure shows that if there is a heavy load on the device and too much current (I) is being taken from it, the output voltage V drops to zero and therefore no power is generated. On the other hand, if no current is being drawn from the device, maximum voltage is yielded, and still no power is generated. As a result, the output load must be adjusted based on the exposure level of the panel to sunlight in order to yield maximum power.

In the design, Atira Technologies utilized switch-mode technology to dynamically modify the load based on the available power generated by the solar panel, so that we may maintain an operational point very close to the Maximum Possible Power Generated (MPPG) window, thus allowing a wider range for the panel to improve efficiency. The figure below depicts the MPPG windows of two different loads.

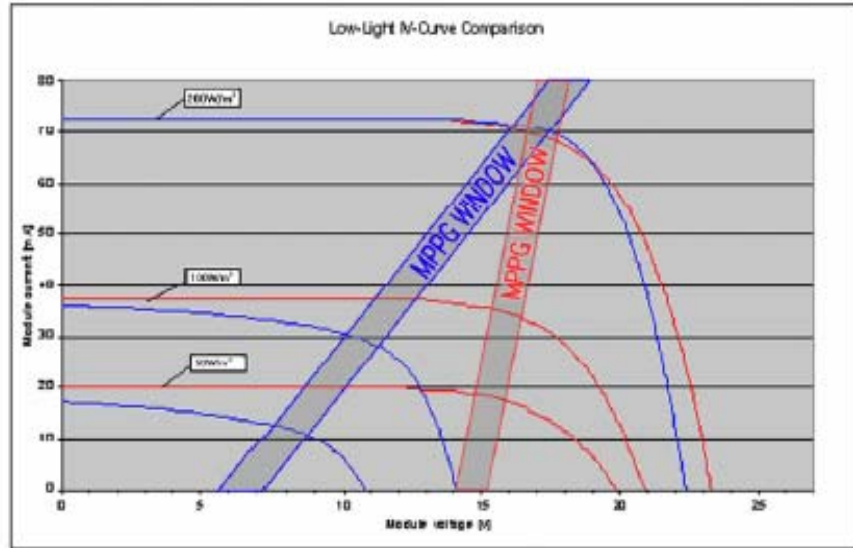


Figure 60. Optimal Charging Window [From Ref 24]

G. CONVERTER DESIGN

The Photovoltaic Power Converter converts the power generated by the solar cells to a DC electrical current to charge the battery. The unique aspect of its design allows usage of the solar panel over an extended range of lighting conditions. The converter designed by Atira consists of circuitry that basically generates an output current from the solar power panel source using switch-mode technology. The control loop is closed around the input voltage to the converter rather than around the output voltage. Consequently, this allows the output voltage to float, only clamped by the loading conditions. That is, if the outputs from multiple units are tied together, the currents will sum. If the outputs are connected to a battery, then the battery's potential will clamp the voltage during charging. This methodology allows all the cells that are producing power to work at their peak efficiency, resulting in overall system efficiency. The circuit also implements other basic conversion and control technology that has existed in the power conversion field. Simple passive and active components were used such as resistors, transistors, capacitors, switches, diodes, and a digital adder. The figure below provided by Atira Technologies shows the circuit design of a novel buck-boost converter specifically designed to track the maximum power point of each panel. The result is a significant increase in the overall satellite available power.

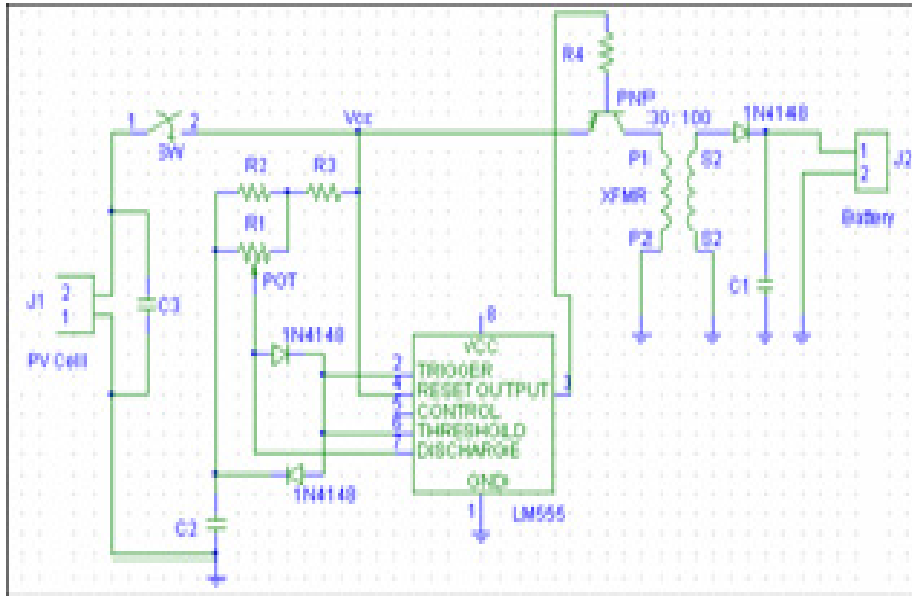


Figure 61. Power Conversion Schematic [From Ref 24]

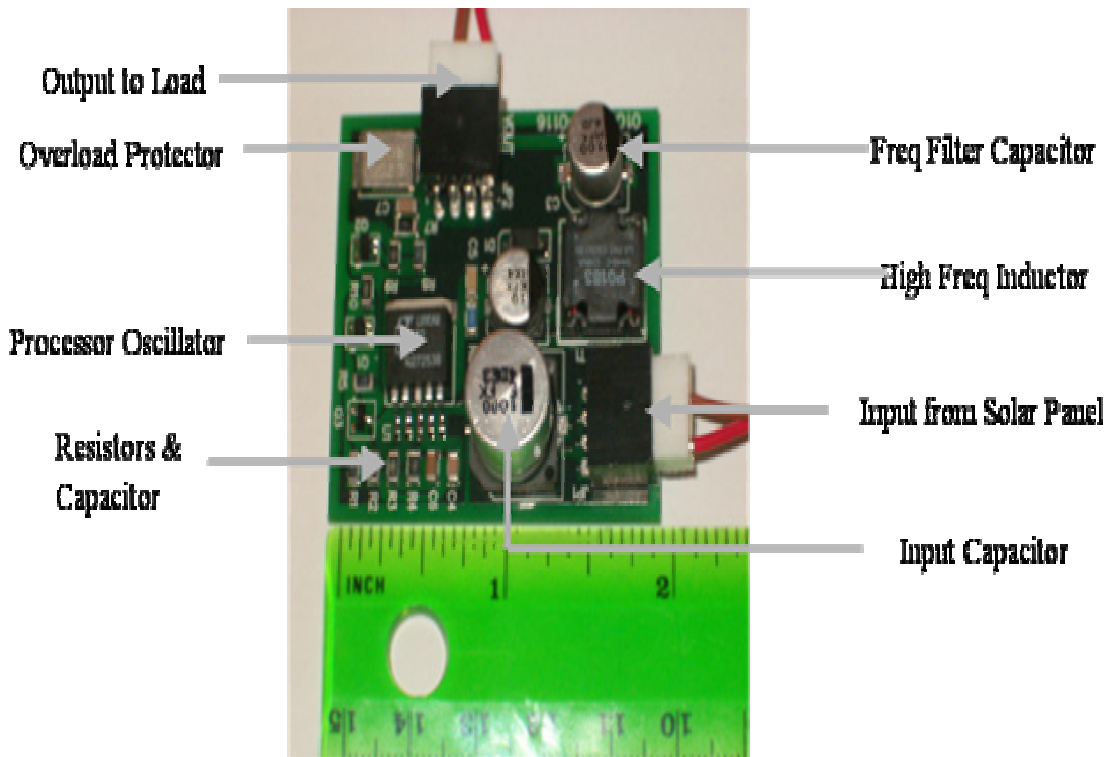


Figure 62. Digital Photograph of the Photovoltaic Power Converter [From Ref 25]

H. SUMMARY

As NPSAT1 is getting ready to launch to perform its various important missions, many technologies can be utilized or improved upon to enhance mission success. One of these technologies is the potential of an outstanding power conversion technology proposed by Atira Technologies, where overall system efficiency can be greatly improved.

As seen from the test results, this converter circuit will be able to provide extra power to complement the main power source onboard NPSAT1. Depending on specific requirements, this circuit can be as small as 5cm x 5cm wide and connected to either a panel or even to each of the rings aboard NPSAT1. In addition, this back-up power source can provide up to 12 Vdc, with 80W continuous and 150W peak of power. As a potential back-up power source, the converter will be able to provide extra power to complement the main power source to support all the missions the satellite is intended to perform. Further, the converter utilizes switch-mode technology along with proven simple conversion and control technology in its circuitry in order to minimize maintenance and repair.

Overall, with the back-up power source, the system power efficiency on board NPSAT1 can be expected to improve up to 20%. Obviously, this would allow for longer time on orbit for the satellite so that it could extend its missions.

VII. CONCLUSION

A. INTRODUCTION

For this final chapter of the research, we will satisfy the primary and secondary research questions listed in the first chapter, including recommendations for further research.

B. CONCLUSIONS

1. Primary Research Question:

- a. *In addition to improved efficiency, reliability, and cost effectiveness, what other aspects of this circuit design that will benefit the military in low wattage applications such as night vision devices, notebook computers, GPS units, and communication suites?*

It became apparent that all tests conducted have shown that the PVPC produced more power than the standard system without the technology. Also, the fact that it was able to transform what was previously unusable power into usable power is a significant capability improvement by itself to the current technology for battery charging.

The capability of charging various batteries using a single panel also exists with the use of this technology. Additionally, the PVPC's ability to provide more power to overcome the battery voltage potential during periods of low light conditions is another major advantage of the PVPC circuit over the standard solar power system.

2. Secondary Research Questions:

- a. *In addition to military applications, what are the potential benefits that this circuit would generate if employed in space applications, such as the NPSAT1 satellite?*

The NPSAT1 will soon be launched to perform its various important missions and the potential of an outstanding power conversion technology of the PVPC can greatly improve the overall system efficiency of the satellite. The test result shows that this converter can provide extra power to complement the main power source of NPSAT1 to support all the missions the satellite is intended to perform. The back-up power source can provide up to 12 Vdc, with 80W continuous and 150W peak of power.

Furthermore, the converter utilizes switch-mode technology along with proven simple conversion and control technology in its circuitry in order to minimize maintenance and repair. Overall, with the back-up power source, the system power efficiency on board NPSAT1 can be expected to improve up to 20%. Obviously, this would allow for longer time on orbit for the satellite so that it could extend its missions.

A published paper written by S. Michael and the author was presented at the 23rd AIAA International Communications Satellite Systems Conference in Rome, Italy on September 2005 entitled, “Improving Spacecraft Power Using an Advanced Maximum Power Tracking Circuit Onboard the Naval Postgraduate School Satellite: NPSAT1”[36].

C. RECOMMENDATIONS

1. Recommendations for Future Research

- Student conducts further analysis to improve on the converter efficiency during a full complement of the solar energy due to the skew result in LM-3 Programmable Fixed Load test.
- Implement the technology on a spacecraft to verify the expected benefits.
- Design a panel for UAV and show total available power for further analysis of the efficiency.
- Build and design the PVPC converter into a chip to reduce the size and possibly install it, one for each sub-panel and show the result.

LIST OF REFERENCES

1. B. W. Lo, "Evaluation and Testing of the Naval Postgraduate School Satellite (NPSAT1) Solar Cell Measurement System," September 2004.
2. Fahrenburch, A.L, and Bube, R.H., "*Fundamentals of Solar Cells – Photovoltaic SolarEnergy Conversion*," Academic Press, Inc., New York, 1983.
3. Jet Propulsion Laboratory, "Solar Cell Array Design Handbook – Volume 1," National Aeronautics and Space Administration, 1976.
4. Oriel Instruments, Introduction to Solar Simulators, [http://www.newport.com/store/product.aspx?id=5759&lang=1&Section=detail]. Last accessed August 2005.
5. Green, M.A., "*Solar Cells: Operating Principles, Technology, and System Applications*" Prentice-Hall, New Jersey, 1982.
6. Hu, C., and White, R.M., "*Solar Cells – From Basic to Advanced Systems*" McGraw-Hill, New York, 1983.
7. Viswanathan, C.R., "*An Introductory Text on Basic Semiconductor Devices*," Course Notes at the University of California, Los Angeles, 1995.
8. Mazer, J.A., "*Solar Cells: An Introduction to Crystalline Photovoltaic Technology*," Kluwer Academic Publishers, Boston, Massachusetts, 1997.
9. Sedra, A.S., and Smith, K.C., *Microelectronic Circuits*, 4th ed., Oxford University Press, New York, 1998.
10. Michael, S., Course Notes for EC3230 (unpublished), Naval Postgraduate School, Monterey, California, March 2005.
11. Michalopoulos, P., *A Novel Approach for the Development and Optimization of State-of-the-Art Photovoltaic Devices Using Silvaco*, Master's Thesis, Naval Postgraduate School, Monterey, California, March 2002.
12. American Solar Challenge, <http://www.formulasun.org/education/seles12.html>, last accessed August 2005.
13. Photovoltaic Fundamental, <http://www.fsec.ucf.edu/pvt/pvbasics>, last accessed August 2005.
14. The Basics of Photovoltaics, <http://www.poweriseverything.com/solar-power-txt.html>, last accessed August 2005.

15. Mohan, Undeland and Robbins, *Power Electronics: Converters, Applications and Design*, 2nd ed., Wiley, 1995.
16. [http://www.powerdesigners.com/InfoWeb/design_center/articles/DC-DC/converter.shtml], last accessed August 2005.
17. R. W. Erickson, Department of Electrical and Computer Engineering, University of Colorado. Boulder, CO 80309-0425
18. Fang Z. Peng, *Introduction to Power Electronics*, Department of Electrical and Computer Engineering, Michigan State University, [http://www.egr.msu.edu/~wanglanj/PE_INTR1-3.pdf], last accessed September 2005.
19. J. Stout, *Ubiquitous Power; Opportunities and Benefits of the Photo-Voltaic Power Converter for the Individual War Fighter*, MBA Professional Report, Naval Postgraduate School, December 2004.
20. Hamilton, Jason A., Sablan, Steve A., Whiteker, James S, *Logistical Impact Study of Photovoltaic Power Converter Technology to the United States Army and United States Marine Corps*, MBA Professional Report, Naval Postgraduate School, Monterey, CA: December 2004.
21. M.A. Dornheim, "Perpetual Motion", *Aviation Week & Space Technology* New York: Jun 27, 2005., Vol. 162, Iss. 26, p. 48-52
22. [<http://uav.wff.nasa.gov/>], last accessed August 2005.
23. S. R. Mitchell, "A Comparative Study of the Prospective Solar Cells for NPSAT1," September 2002.
24. David A. Besser, "Photovoltaic Power Conversion Technology," December 2004 (revised).
25. Ansley, Steven R. and Phillips, Lewis H., "The Photovoltaic Power Converter: A Technology Readiness Assessment" (MBA Professional Report, Naval Postgraduate School, June 2005).
26. C. Austin, R Borja, and J Phillips, "A Study Examining Photovoltaic (PV) Solar Power as an Alternative for the Rebuilding of the Iraqi Electrical Power Generation Infrastructure" (MBA Professional Report, Naval Postgraduate School, June 2005).
27. Boeing Spectrolab, "Photovoltaic Products Data Sheets," [<http://www.spectrolab.com/prd/space/cell-main.asp>], last accessed July 2005.

28. Sakoda, Dan and Horning, James A., Overview of the NPS Spacecraft Architecture and Technology Demonstration Satellite, NPSAT1, Naval Postgraduate School, Monterey, CA. May 2002.
29. D. Sakoda, "Overview of the Naval Postgraduate School Petite Amateur Navy Satellite (PANSAT)," 13th AIAA/USU Conference on Small Satellites, August 23-26, 1999.
30. CAD Models and System diagrams by Dan Sakoda, NPS Space Systems Academic Group.
31. B. W. Lo and S. Michael, "Evaluation and Testing of the Solar Cell Measurement System Onboard The Naval Postgraduate School Satellite NPSAT1", Proceedings of the 22nd AIAA International Communications Satellite Systems Conference, Monterey, CA, May 9-12, 2004.
32. NPSAT1 Design Overview.
[<http://www.sp.nps.navy.mil/npsat1/technical/NPSAT1.htm>], last accessed August 2005.
33. Ultralife Batteries.
<http://www.ultralifebatteries.com/datasheet.php?ID=UBBL02>], last accessed August 2005.
34. Improved Triple Junction Solar Cells.
[<http://www.spectrolab.com/DataSheets/TNJCell/tnj.pdf>], last accessed August 2005.
35. Solar Energy Company.
[www.solengy.com/pages/whitepapers.html], last accessed July 2005.
36. S. Michael and R. Fernandez, "Improving Spacecraft Power Using an Advanced maximum Power Tracking Circuit Onboard the naval Postgraduate School Satellite: NPSAT1", Proceedings of the 23rd AIAA International Communications Satellite Systems Conference, Rome, Italy, September 2005.

THIS PAGE INTENTIONALLY LEFT BLANK

INITIAL DISTRIBUTION LIST

1. Defense Technical Information Center
Ft. Belvoir, Virginia
2. Dudley Knox Library
Naval Postgraduate School
Monterey, California
3. Chairman, Code EC
Department of Electrical and Computer Engineering
Naval Postgraduate School
Monterey, California
4. Professor Sherif Michael, Code EC/Mi
Department of Electrical and Computer Engineering
Naval Postgraduate School
5. Associate Professor Robert W. Ashton, Code EC/Ah
Department of Electrical and Computer Engineering
Naval Postgraduate School
Monterey, California
6. Atira Technology
Los Gatos, California
7. LT Randyll R. Fernandez, USN
Oxnard, California